**Carlos Miguel
Vieira Correia**

**Recovery of Reprocessed Thermoplastic Properties
for Closed-Loop Recycling using Fused Filament
Fabrication**

Recuperação das Propriedades de Termoplástico Reprocessado para Fabrico por Filamento Fundido em Ciclo Fechado

Universidade de Aveiro
2021

Carlos Miguel
Vieira Correia

Recovery of Reprocessed Thermoplastic Properties for Closed-Loop Recycling using Fused Filament Fabrication

Recuperação das Propriedades de Termoplástico Reprocessado para Fabrico por Filamento Fundido em Ciclo Fechado

"Fools make researches and wise men exploit them - that is our earthly way of dealing with the question, and we thank Heaven for an assumed abundance of financially impotent and sufficiently ingenious fools"

- H.G. Wells in "A Modern Utopia"

o júri / the jury

presidente / president

Prof. Doutora Mónica Sandra Abrantes de Oliveira Correia
Professora Auxiliar com Agregação da Universidade de Aveiro

Prof. Doutora Mariana Doina Banea
Professora Adjunta do Centro Federal de Educação Tecnológica Celso Suckow da Fonseca - Cefet/rj (Arguente)

Prof. Doutor Victor Fernando Santos Neto
Professor da Universidade de Aveiro (orientador)

Doutora Idalina José Monteiro Gonçalves
Investigadora na Universidade de Aveiro (co orientador)

abstract   Additive manufacturing technologies based on Material Extrusion (ME) have been growing, gaining popularity and maturity in the plastic processing sector. In this context, it is a major concern to establish a closed-loop plastic production system which allows to maximize the value and shell-life of the feedstocks used in these kind of manufacturing technologies, contributing to decrease their ecological footprint. Regarding ME or Fused Filament Fabrication (FFF), a possible closed-loop recycling scheme would consist of processes for material collection, preparation, and filament extrusion in order to produce 3D printing feedstocks that fits with the FFF requirements and allows to achieve new value-added parts. However, there are challenges to overcome related to the quality and performance of the recycled materials, since, after mechanical recycling, the molecular degradation of thermoplastics causes a shift on their properties, and, therefore, on their processability. In this work, it was hypothesized that the incorporation of chain extenders (CE) during the reprocessing cycle would allow to overcome these drawbacks. To attest this conjecture, the influence of 1,3-Bis(4,5-dihydro-2-oxazolyl)benzene (PBO), a functional additive used as a CE for polylactic acid (PLA) and PLA-based blends, at a fixed concentration (1%, w/w) on mechanical, thermal, and rheological properties of recycled PLA-based filaments was studied, using virgin PLA-based material as control. PBO was able to partially recover the mechanical performance of recycled PLA-based systems, as reflected by an increase in both tensile modulus and tensile strength of the filament specimens. However, these results did not corroborate with the evolution of the material's melt strength, monitored by the melt flow rate (MFR), since PBO increased the MFR of recycled PLA-based formulation. This behavior may be related to the low interaction established between PBO and PLA, as observed by Fourier transform infrared spectroscopy (FTIR). From the printability point of view, it was observed that the brittleness of each studied formulation remained as the major constraint for successfully establish a closed-loop recycling scheme for FFF.

palavras-chave   Manufatura Aditiva; PLA; Reciclagem de Termoplásticos; Extensão da Cadeia do PLA; PBO; Degradação Termo-mecânica

resumo   As tecnologias de manufatura aditiva baseadas em extrusão de materiais termoplásticos como o Fabrico por Filamento Fundido (FFF) têm-se destacado, ganhando popularidade e maturidade no contexto da indústria de processamento de plásticos. Desta forma, o esbelecimento de modelos de produção de plásticos em ciclo fechado é uma área de extremo interesse, pois possibilita maximizar o valor dos materiais utilizados neste tipo de tecnologias de fabrico, contribuindo igualmente para a redução do seu impacto ambiental. No contexto do FFF, um possível sistema de reciclagem em ciclo fechado consiste nos processos de recolha, preparação dos materiais e extrusão de filamento com o objetivo de conformar o material de forma a que este possa cumprir os requisitos da tecnologia, possibilitando a produção de componentes de valor acrescentado. Contudo, existem um conjunto de desafios associados à qualidade e performance dos materiais reciclados, dado que, após a aplicação dos processos de reciclagem mecânica, a degradação ao nível molecular a que os materiais termoplásticos são sujeitos irá provocar uma alteração nas suas propriedades e, consequentemente, nas suas condições de processamento. Neste estudo, é colocada a hipótese de, através da utilização de extensores da cadeia (EC) polimérica durante o ciclo de reprocessamento, ultrapassar as limitações relacionadas com a excessiva degradação do material. Neste sentido, a influência do 1,3-Bis(4,5-dihydro-2-oxazolyl)benzene (PBO), um aditivo funcional utilizado como extensor da cadeia para o ácido poliláctico (PLA) e formulações baseadas em PLA, a uma dada concentração (1%, m/m), nas propriedades mecânicas, térmicas e reológicas do material foi estudada, utilizando PLA virgem como material de controlo. A incorporação do PBO permitiu a recuperação parcial das propriedades mecânicas dos sistemas baseados em PLA reciclado, refletido pelo aumento do módulo de elasticidade e da tensão de rotura nas amostras de filamento. No entanto, estes resultados não são comprovados pela evolução da fluidez do material, monotorizada através do índice de fluidez (MFR), dado que o PBO contribuiu para o aumento do MFR das formulações baseadas em PLA reciclado. Este comportamento pode estar relacionado com a interação limitada entre o PBO e o PLA, observada através da espetroscopia de infravermelho por transformada de Fourier (FTIR). Na perspetiva da capacidade de impressão, o comportamento frágil do material foi identificado como a maior limitação ao estabelecimento de um sistema de reciclagem em ciclo fechado para aplicações na tecnologia de FFF.

Contents

List of Tables

Intentionally blank page.

List of Figures

Intentionally blank page.

Part I

Introduction and background

Chapter 1

Introduction

1.1 Contextualization

The pathway into the future will require a smarter management of both materials and energy in order to reach a sustainable usage of the planet's limited resources. In this context, waste management, and plastic recycling in particular, constitutes one of the most important and interesting challenges for achieving a sustainable society. Although plastics were only introduced at large-scale production in the mid-twentieth century, their versatile properties and easy processing has led them to be prime materials with a wide range of applications [1]. However, their dependency on fossil feedstocks and improper disposal, which leads to their accumulation on land and marine environments represents a negative impact on natural ecosystems, thus being a subject of great concern from social, academic, and governmental perspectives [1].

As an alternative to the petroleum-sourced plastics, bio-based and biodegradable polymers such as polylactic acid (PLA) have been gathering much attention since they can be produced from renewable sources and provide a composting-based end-of-life disposal pathway [2]. Nonetheless, several authors state that the application of compostable polymers in single use commodities is unsustainable, hence their recyclability should be addressed in order to obtain an extended value for these materials [2; 3]. In this context, different recycling approaches have been reported for PLA-based materials, particularly the chemical and mechanical recycling [4]. A mechanical recycling-based system is composed from the processes of sorting, washing, grinding, and re-compounding of the plastic waste materials in order to provide feedstock for further (re)processing and can be either applied to post-industrial (PI) or post-consumer (PC) plastic waste streams in closed-loop or open-loop recycling schemes [5].

The main challenge for introducing recycled feedstocks in the plastics manufacturing cycle is related to their degree of mixing with different chemical classes of plastic polymers and other contaminants (particularly when handling complex mixtures from post-consumer waste streams) and their degree of degradation caused by the processing and service-life [6]. Polymers are prone to degrade due to the processing and environmental conditions that they are exposed, decreasing their molecular weight and mechanical, rheological, and thermal performance [6]. Currently, different strategies for upgrading degraded polymers have been addressed in the literature, particularly polymers restabilization; copolymerization; incorporation of a certain percentage of virgin polymers

together with the recycled feedstocks; and rebuilding of the cleaved molecular chains [2; 3; 6].

Rebuilding of degraded polymers through the application of functional additives such as chain extenders has been proved to be an interesting approach for enhancing the properties of recycled PLA [2]. Chain extenders (CE) are able to reconnect the cleaved polymeric chains, thus being able to increase the molecular weight of a polymer without sacrificing its mechanical and thermal performance and, therefore, allowing to fulfill the requirements of a wide range of polymer processing techniques, including additive manufacturing technologies [7; 8].

Additive Manufacturing (AM) is the general term for a bundle of technologies which are based on the creation of 3D objects by successive addition of material, in opposition to the conventional subtractive manufacturing technologies such as machining, where a 3D part is created by subtracting material from a solid block [9]. Within AM, Material Extrusion (ME), often designated as Fused Deposition Modeling (FDM) or Fused Filament Fabrication (FFF), is a process in which the material is selectively deposited through a nozzle to create 3D parts in a layer-by-layer methodology and represents the most widely spread AM-related technology, available for both industrial and consumer-manufacturer applications [9; 10; 11].

The feedstocks generally used in FFF are thermoplastics such as acrylonitrile butadiene styrene (ABS) and PLA in the shape of a thin filament with a diameter range between 1.75 mm to 3 mm [11]. Particularly, PLA has been the material of choice for most FFF-based applications, since it has a low melting temperature and it is of easy processing. Moreover, several commercial filament manufacturers are already moving towards a recycled polymer-based production such as RE-PET3D [12], Filamentive [13], Reflow [14] and Tucab [15] which offer filaments made by recycled PLA and polyethyl benzene-1,4-dicarboxylate (PET), in order to promote sustainability among the consumers and enthusiasts. Additionally, the development of desktop-range filament extruders provides the opportunity for extended recycling of additive manufacturing by-products as well as research and development (R&D) of new recycling procedures based on the knowledge of both material science and processing equipment areas, allowing for the formulation of circular and sustainable value chains, such as the distributed recycling via additive manufacturing (DRAM) waste management strategy [16; 17].

1.2   Objectives

The main objective of this work was to establish a closed-loop recycling procedure for additive manufacturing technologies, particularly for the extrusion-based technologies such as FFF. In this context, multiple cycles were employed to an industrial-grade PLA, monitoring the different processing steps effect on the structure, mechanical, and thermal properties, as well as on the processability of the recycled PLA-based samples. Furthermore, the incorporation of a fixed amount of a functional chain extender was employed either in the virgin feedstock and in the recycled one in order to understand to which extent the rebuilding of the degraded polymeric chains could help to recover the PLA-based material properties, providing a pathway for the production of functional components with recycled PLA.

1.3 Document structure

The subsequent sections are divided into four main chapters: (2) Literature review, (3) Experimental work, (4) Results and Discussion, and (5) Conclusions and future works.

The *Literature review* chapter aims to present theoretical concepts and definitions as well as to summarize the knowledge gathered from previous works about additive manufacturing, plastic recycling, upgrading strategies, and to establish the main limitations of a closed-loop recycling scheme based on FFF. This chapter is, within itself, divided in four different sections. Section 2.1 is related to additive manufacturing and presents an overview of the technology, the materials employed, the main process parameters, and ends with the description of the processes which allow for the production of thermoplastic filaments both at an industrial and laboratory scale. Further, Section 2.2 and Section 2.3 are related to the reprocessing of plastic materials, particularly by mechanical recycling pathways and upgrading strategies. Section 2.4 presents the main challenges for establishing a closed-loop recycling scheme using FFF technology as identified in the literature.

Chapter 3, entitled *Experimental work*, presents all the experimental procedures adopted in order to obtain valuable data about the evolution of the material's performance and processing conditions as a function of the number of cycles employed. This chapter encompasses one distinct section designated as *Materials and Methods* which is, divided in three subsections. Subsection 3.1.1, *Fabrication of samples*, aims to explain how the samples for monitoring the property profile and processability of each formulation were obtained, as well as to describe the experimentation stage of the experimental work, which was used to understand, within the available equipment and processing conditions, which ones were suitable for employing the proposed methodology. Furthermore, subsection 3.1.2, *Processing equipment*, was used to extensively detail the processing equipment and conditions that were used over the course of this research, whilst subsection 3.1.3, *Evaluation of properties*, was dedicated to present the equipment and testing conditions which were used to gather data to be further discussed.

Chapter 4, designated as *Results and discussion* is related to the presentation of results and their discussion against the knowledge gathered from previous works on the same subject.

Chapter 5, designated as *Conclusions and further work* comprises the final remarks of the experimental work as well as the discussion of the advantages and limitations of the proposed methodology, when compared to the previous studies. Additionally, possible research paths to be addressed in future work are anticipated, particularly in order to expand the methodology to a wider extent and provide a pathway for the production of functional 3D parts based in recycled-recovered polymers.

Intentionally blank page.

Part II

Literature review

Chapter 2

Literature Review

In order to accomplish the main objective of this research work, which was establishing a closed-loop recycling procedure for additive manufacturing technologies, the technical background related to these manufacturing technologies is to be set. In this context, this chapter starts by describing extrusion-based AM hardware and software apparatus, materials, process parameters and the manufacturing cycle involved in the production of thermoplastic filaments, the main feedstock material for Fused Filament Fabrication.

Moreover, the research questions which arise from the main objective of this research work, particularly, the incorporation of recycled materials into the manufacturing cycle, at a first stage, and the hypothesis of recovering the material's performance via the addition of functional chain extenders are addressed according to the state-of-art literature. In this context, recycling procedures, degradation mechanisms characterization, upgrading strategies, and challenges and opportunities regarding the establishment of closed-loop recycling procedures for PLA-based formulations, as identified in the literature, are presented in order to provide sufficient knowledge to be compared to the data produced in the experimental work conducted over the course of this study.

2.1 Fused Filament Fabrication (FFF)

Fused Filament Fabrication (FFF) is an AM technique that makes use of material extrusion, usually a thermoplastic polymer in the form of a thin filament, through a heated nozzle to create 3D objects in a layer-by-layer methodology [9]. As for today, FFF represents the most widely spread AM-related technology, since most of the industrial and household 3D printers fall into this category [10].

The main advantages of FFF are related to the low initial investment and easy operation associated with the machines, as well as the wide range of available materials which go from commodity thermoplastics, like PLA or polypropylene (PP), to engineering and high-performance materials, such as polycarbonates and polyether ether ketone (PEEK), respectively [11]. Under certain processing parameters, FFF technology is able to produce components 85% as strong as their molded counterparts [11]. However, the downsides associated with this technology include limitations on the accuracy and available precision; anisotropic nature of the build; and requirement of post-processing operations in most of its applications, in order to assure the functional and aesthetic

properties of the obtained parts [10].

For generating a 3D part through FFF, one must undergo a defined number of steps, starting with the digital model of the physical object which can be obtained from any computer-aided design (CAD) software available on the market, such as SolidWorks, Catia, Rhino and Inventor, among others [18]. The digital design must then be exported as a STL file, a file format which describes the surface geometry of a tridimensional object by using a mesh of triangles or "facets" [18]. The communication between the digital file and the machine's hardware is either intermediated by a slicing software, such as Cura and Simplify3D, or directly by the CAD software. This step aims to configure the object model to be processed by defining the machine specifications (nozzle diameter, for example), material selection [18], and it is also responsible for separating the tessellated model into layers and generating a G-code that includes the coordinates and all the configurable process parameters which will be discussed in a further section.

When the G-code with the 3D model information is uploaded into the machine, the nozzle is heated up to the melting temperature of the raw material and the filament is fed into the print head to be melted. The print head is able to move spatially in the X, Y, and Z directions, depositing the material to create the determined layers [18]. When a layer is finished, the print head moves slightly up and the next layer is deposited, a process that it is repeated until the 3D build is completed [18]. Due to this manufacturing strategy, whenever the model presents overhangs shallower than 45° from the horizontal plane, auxiliary support structures must be built in order to guarantee their feasibility [18]. These supports can be either printed in the same material of the build or in a dissolvable thermoplastic like high-impact polystyrene (HIPS) [18]. The latter option, however, requires the machine to be equipped with a dual extruder head [18]. The presence of support structures will always compromise the surface quality of the 3D printed parts [18].

The fundamental components of a FFF machine are the print head and the print platform, as well as the machine's operational coordinate system and mechanical nature (Figure 2.1). The print head is composed by the extruder unit (Figure 2.1 - left) which is responsible for moving and processing the filament. The extruder (Figure 2.1 - right) can be identified as a direct drive extruder or a Bowden extruder, whether the cold end which drives the filament is mounted directly on the print head or in the machine's frame, respectively [19].

On the other hand, the build platform (Figure 2.1 - left) is a thin plate whose primary function is to provide a flat surface for the bottom layer to be built upon [20]. The build plate or print bed is often made in aluminum since it has good thermal conductivity and allows a faster spreading of the heat throughout the printing area [20]. For enhancing the bottom layer's finish, a glass plate is often placed above the aluminum heated platform [20]. Glue stick, painter's tape or some varieties of hairspray are also employed for enhancing the bottom surface finish and adhesion to the build plate [20].

Aside from the print head and build platform, the operational coordinate system and mechanical nature define the FFF machine configurations [21]. The machine coordinate system can be either cartesian or polar. A typical FFF machine makes use of a three-axis cartesian system to determine the position and direction of the printing head and it is composed by square or boxlike frames equipped with linear rails [21]. This
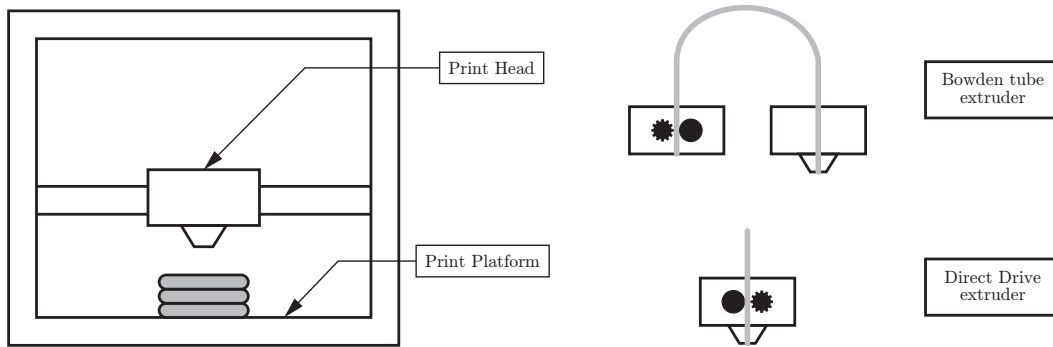
Figure 2.1: Eschematization of the main components of an FFF machine (left) and the hardware distinction between a Bowden and Direct Drive extruders (right).

Figure 2.2: Example of different types of FFF machine configurations: cartesian (Creality3D Ender3 – left), delta (Monoprice Delta Pro – center/left), polar (Sculpto PRO2 – center/right) and SCARA-based (KUKA robotic arm 3D printer – right).

configuration represents an economic approach, which is simple to understand and easy to upgrade or fix. However, its large and heavy frame represents a constraint on the print velocity and build height [21].

Other examples of systems that rely on the cartesian coordinate system are the Delta configuration, which makes use of arms rather than fixed axes achieving faster print rates, and the SCARA-based printers, where the print head is driven by a robotic arm, providing faster and versatile movements [21]. Machines based on the polar coordinate system are also available. These types of machines typically make use of a single arm assisted by a spinning round print bed, but do not achieve high quality prints and are often too slow [21]. These different configurations of the FFF machines are presented on Figure 2.2.

2.1.1   Materials

The most common polymers used within the FFF technology are ABS and PLA [11]. ABS was one of the first thermoplastics used in industrial 3D printers and allows the production of tough and durable builds that can withstand high temperatures [22].

On the other hand, PLA appears as the default filament of choice for most extrusion-based 3D printers because it can be processed at low temperature, achieving interesting builds with good dimensional accuracy at a low-cost [23]. Also, since PLA is derived from crops such as corn and sugarcane, it is a renewable and biodegradable thermoplastic, which minimizes its net environmental impact [23].

Other thermoplastics typically used in injection molding such as PET and PP, are also employed in FFF, enhancing certain properties of the builds like weather resistance, surface finish, and density [23]. For more demanding applications, polyamides (Nylon/PA) and polycarbonates are also employed [23]. However, these better performance materials are associated with higher processing temperatures, increasing the likelihood of warping and distortion of the 3D parts due to differential cooling, and are often associated with industrial-grade machines that provide greater control over the print environment [11].

The 3D printing materials market is expected to keep growing for the upcoming years, as new companies are investing on the development of new materials and machine manufacturers are moving towards an open-source model rather than a proprietary one [24]. In 2020, it was estimated that 1,095 different types of polymers were available for 3D printing, with 38% of them being developed for extrusion-based technologies such as FFF [24]. An increasing demand for high-performance polymers is also trending, which provides the opportunity for introducing more complex materials, such as composites [24].

3D printing composites are often comprised by a short or continuous fiber reinforcement blended within a polymeric matrix for enhancing the strength and stiffness of the materials, when compared with the non-reinforced counterparts [25]. There is a wide range of reinforcement materials that can be incorporated into the FFF manufacturing process, such as carbon nanotubes (CNT), graphene, copper, iron fillers and continuous or short fibers of carbon (CF), glass (GF), and Kevlar [26]. However, the incorporation of short fibers into 3D printing filaments requires a hardened steel nozzle in order to resist the abrasive nature of the fiber strands, while the application of continuous fibers adds complexity to the process since it requires an independent extrusion circuit for fiber strands deposition [25]. There are also concerns related to the end-life usage of this category of materials since they are often not properly recycled [27]. Table 2.1 presents the most relevant properties associated to the materials employed in FFF technology.

2.1.2 Processing parameters

Apart from the raw materials, machine specifications and configurable process parameters also perform an important role on the outcome of FFF 3D printed parts. In fact, in this manufacturing process it is often the adhesion between layers that defines the strength of a component, rather than the raw material itself [10].

In this context, a lot of research has been conducted regarding the optimization of processing parameters for achieving functional 3D printed parts. To build a part for strength, monitoring the extrusion temperature and cooling of the part is crucial, since despite the materials being able to withstand stress, under inadequate printing conditions, strings of materials do not bond correctly with each other, which results in fragile 3D structures that crack even when exposed to mild compression/traction/impact conditions [28].

Table 2.1: Physical properties of raw materials for FFF technology [30].

Designation	ABS	PLA	PP	PET(G)	Polycarbonate	PA	CF composite
Tensile strength (MPa)	40	65	32	53	72	40-85	45-48
Max. temperature (°C)	98	52	100	73	121	80-75	52
Density (g/cm³)	1.04	1.24	0.90	1.23	1.20	1.06-1.14	1.30

Besides temperature control, layer height, nozzle material and diameter, material feed rate, retraction, and print speed (Figure 2.3 - left), if not set according to the feedstock material being used, type of machine, object design, and expected performance, can cause undesirable functional and aesthetic properties, such as color change spots and rough surfaces [28]. Dimensional accuracy is also problematic as the thermoplastic polymers tend to shrink unevenly and warp due to differential cooling [28]. A strict control of the bed temperature and the use of machine enclosures for real-time monitoring of temperature and humidity can help to avoid the 3D part deformation and inaccuracies, such as staircase effect, which is often associated to extruding-based 3D printed objects [28].

Build orientation, raster width, raster angle and infill density (Figure 2.3 - right) also contribute for the 3D printed parts mechanical behavior [29]. When processing ABS through the FFF technology, an increased nozzle diameter enhances the strength between layers by reducing the presence of voids, which positively affects the tensile strength of the 3D printed parts [29].

On the other hand, PLA tensile strength is mainly affected by the raster angle, raster width, and layer height. For optimizing the tensile properties of PLA-based 3D printed parts, the definition of the raster angle must be set so the applied load is mainly borne by the filament in the longitudinal direction rather than the bond between layers [29]. Maximum raster width and minimum layer height provide an increased layer adhesion and are both determined by the machine's setup, with the recommended layer height being set as 25% to 50% of the nozzle's diameter [28]. PLA-based 3D printed parts can also be annealed as a post-processing procedure for enhancing their strength [29].

Other commonly used thermoplastic filaments such as Nylon and PEEK behave similarly to the process parameters as ABS and PLA [29]. However, when processed by the FFF technology, neither of these materials can achieve mechanical properties as competitive as the other conventional manufacturing methods [29].

2.1.3   Monofilament manufacturing

FFF manufacturing technology relies on a round-shaped thermoplastic filament similar to the one used in grass string-trimmers as feedstock material [11]. This synthetic filament, which has a diameter within 1.75 to 3 mm, is produced from polymer pellets by a plastic extrusion process to achieve the desired shape, dimensions, and physical properties.
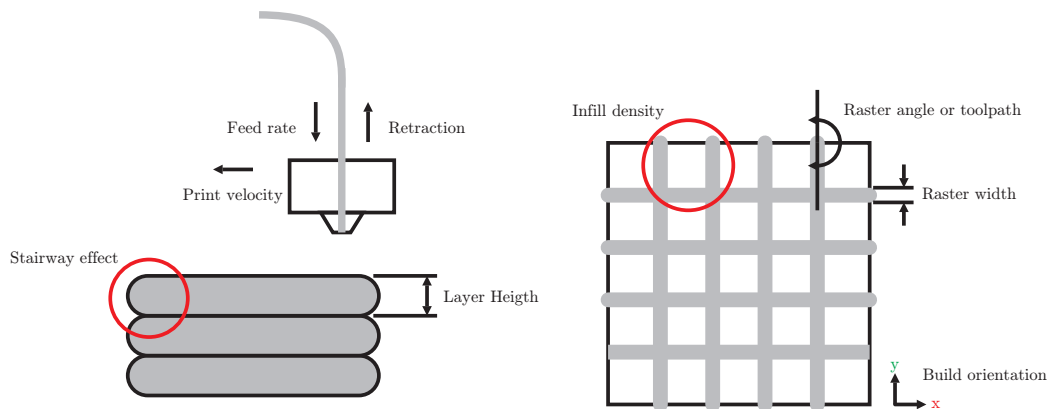
Figure 2.3: Representation of the main processing parameters that affect the properties of 3D printed parts obtained by FFF.

Extrusion process

Prior to the extrusion process, the granulated polymer is combined with additives on a blender for improving its processability and enhancing certain properties such as color and wear resistance [31]. Since some categories of thermoplastic polymers, such as PLA, tend to be highly hygroscopic, a drying stage is usually performed before the extrusion step, so the absorbed moisture can be removed, thus preventing manufacturing defects and preserving the material's performance [31].

Afterwards, the polymeric mixture is fed into an extruder equipment. Extrusion is one of the most widely used plastic manufacturing technology, based on the consecutive operations of heating, cooling, and drawing a polymeric material through a specific die to form several types of products such as films, pipes, cables, and profiles [31]. Monofilament-making industries usually employ single screw extruders to form thin round-shaped profiles with residual cross-sectional areas when related to its length [32].

A single screw extruder is comprised by a screw and barrel units that interact together to convoy, plasticize, and then push the material through the specified die or spinneret [31]. The screw is rotated at a predetermined speed, driven by an electric motor and gearbox, whereas heating and cooling elements that are attached to the barrel provide different thermal stages that are set according to the processed material [31].

When the extrudate leaves the die, it has to be subjected to a multi-stage cooling chamber where the desired shape is to be set [33]. For manufacturing FFF filament, usually two cooling chambers are employed, with the first being full of warm water as coolant, which helps to provide the filament a clear round shape rather than an oval shape, that is often critical for the FFF process [33]. The second cooling stage works with room temperature water as coolant and goes as long as it is necessary for the thermoplastic filament to cool and permanently set its shape [33].

The spinneret employed in the monofilament manufacturing has usually a circular shape and its land length tend to be 2 to 5 times the filament's desired diameter [32]. However, the final diameter of the filament is determined by the puller speed, rather than

the spinneret's channel dimensions [32]. In this context, decreasing the puller speed will result in a larger filament diameter, while increasing the puller speed does the opposite [32]. A laser micrometer and optical sensors are often used within the extrusion line to provide real-time monitoring of the filament's diameter and cross section shape [32].

Quality control and testing

Quality control of monofilament manufacturing generally relies on the evaluation of geometric and physical properties, such as the diameter and linear mass density consistency, as the main quality indicators [17]. However, assessing the mechanical behavior of the filament is also important to understand the influence of material degradation caused by the extrusion process, which will have a negative impact on the further processing steps [17]. Morphological characterization of the filament can also be performed, particularly to address the compatibility and distribution of elements that are blended within the polymeric matrix, such as additives or reinforcements [17].

Desktop extruders

Several desktop filament extruder lines are also available on the market such as the Filabot EX6, Noztek's filament extrusion system, and Felfil extrusion bundle. These types of equipment have the same functionality as the industrial-grade extruders, hence providing an opportunity for R&D of new raw materials for filaments, as well as evaluating the influence of processing parameters on the final product properties. However, they tend to be quite expensive and do not have the same efficiency as the industrial extruder lines since they neglect the multi-stage cooling which is crucial for producing high quality feedstock for 3D printing.

Reprocessing

Regardless of the extrusion process it is quite common to grind scrap material using a granulator or other appropriate equipment to make granulates that can be fed back into the extruder [32]. However, regrind can affect the performance and processing profiles caused by viscosity and thermal stability shifts on the pristine material [32]. The reextrusion or compounding of recycled polymers allow to make new value-added products, although these strategies may require the addition of heat or UV stabilizers, flame retardants, impact modifiers, or other additives to improve their performance [32]. The trends on thermoplastic reprocessing methodologies, degradation mechanisms characterization, and recovery of their properties will be discussed in the following sections.

2.2   Reprocessing Plastics by Mechanical Recycling

Although plastics were only introduced to large-scale production on the second half of the XX century, they have now outgrown most man-made materials, particularly due to their versatile properties and easy processing, which allows them to be employed in a wide range of products, from packaging to high-technology applications [1; 34]. However, their dependency on fossil feedstock as well as their accumulation on the environment due to improper disposal have been raising awareness about their sustainability [1]. In this context, recyclability of thermoplastics exploration has been a subject of great interest from both academic and governmental perspectives [4; 35].

Thermoplastics are a specific range of polymers constituted by successive linear molecular chains, which have the ability to soften during heating and harden when cooled down, thus being able to be easily reprocessed and reintroduced on the economy as new value-added products [34]. On the thermoplastics recycling hierarchy (Figure 2.4), primary recycling refers to the polymeric product re-usage as-is, whereas secondary recycling or mechanical recycling refers to the re-compounding of the waste stream materials in order to produce new products [34].

Other means of recycling, such as the chemical recycling methodologies, have also been studied as they provide the opportunity to decompose the polymer in their respective monomers and undergo a secondary polymerization process [4]. Biodegradable polymers such as PLA can also be composted, which is described as further example of tertiary recycling [4]. Energy valorization is the ultimate recycling methodology which aims to recover the energetic value of polymeric materials that cannot be further recycled [1; 34]. However, the incineration of this type of materials is associated with the emission of hazardous fumes and chemicals and should only be accounted for avoiding the conventional landfill disposal [5].

2.2.1   Waste stream classification

One of the major limitations of the recycling processes relies on the composition of the waste streams that are fed into the recycling system, particularly their degree of mixing with different chemical classes of plastic polymers and other contaminants, and degradation due to processing and service-life conditions that the materials were exposed [6; 36]. From the scientific literature, these waste streams can be categorized as post-industrial (PI) or post-consumer (PC) plastics, according to their origin [5]. PI waste has the distinct advantage of having a well know composition, often comprised of mono-polymer, uncontaminated streams [5]. In this context, PI waste is considered a higher quality grade of polymer waste, and tends to be recycled to a greater extent [5; 35].

On the other hand, PC waste is composed by a complex mixture of different polymers, which are contaminated by organic elements like food residues and other materials such as adhesives and labels [5]. Moreover, PC plastics often present evident signs of environmental degradation mechanisms, particularly photodegradation, thermo-oxidative degradation, and hydrolytic degradation, and therefore require a more in-depth study to achieve a recycling-based valorization pathway [34; 35].

Thermal analysis, in particular differential scanning calorimetry (DSC), and

```
┌─────────────────┐
│ Extraction of raw │
│ materials       │
└─────────────────┘
         │
         ▼
┌─────────────────┐     ┌─────────────────┐
│ Synthesis of    │◄────│ Feedstock       │
│ polymeric       │     │ Recycling       │
│ materials       │     │                 │
└─────────────────┘     └─────────────────┘
         │
         ▼
┌─────────────┐  ┌─────────────────┐  ┌─────────────────┐
│ Energy      │◄─│ Plastic         │◄─│ Mechanical      │
│ Recovery    │  │ Processing      │  │ Recycling       │
└─────────────┘  └─────────────────┘  └─────────────────┘
         │
         ▼
┌─────────────┐  ┌─────────────────┐  ┌─────────────────┐
│ Landfilling │◄─│ Application and │◄─│ Re-usage        │
│             │  │ service life    │  │                 │
└─────────────┘  └─────────────────┘  └─────────────────┘
         │
         ▼
┌─────────────┐  ┌─────────────────┐
│ Composting  │◄─│ Residue         │
│             │  │                 │
└─────────────┘  └─────────────────┘
```
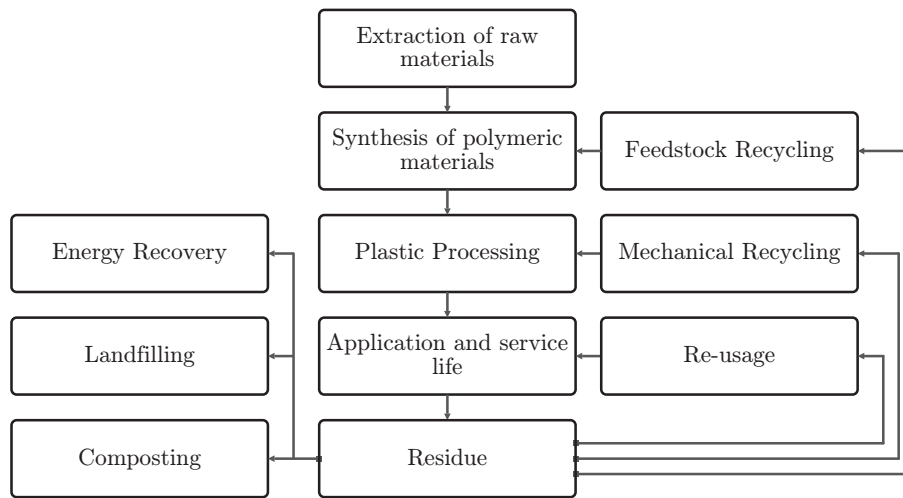
Figure 2.4: Representation of the polymer recycling hierarchy and end-of-life disposal strategies. Adapted from [6].

vibrational spectroscopy techniques such as Fourier-transform infrared spectroscopy (FTIR) are among the most used analytical methods for evaluating the recycled polymer's composition [6; 35; 36].

2.2.2 Mechanical recycling

From a sustainability perspective, mechanical recycling, which is composed by the steps of collecting, sorting, washing, and grinding of the material, represents the most reliable and cost-effective recycling methodology [2]. Also, when handling well-classified waste streams, such as the PI plastics, the steps of sorting and washing can be most times neglected, hence providing an opportunity for enhanced efficiency [5]. However, because of the nature of the processes involved, in particular the application of mechanical shear and thermal cycles during the size reduction and re-compounding steps, thermomechanical degradation is induced on the recycled materials, thus deteriorating their properties and limiting their usability for functional applications, which is sometimes designated as the downgrading of the polymeric waste materials [2; 5].

In this context, reprocessing the plastics by multiple extrusion or injection molding have been common approaches to assess the recyclability of polymers and to study the thermomechanical degradation during processing and mechanical recycling [6]. Pillin *et al.* addressed the reprocessability of poly(L-lactic acid) (PLLA) up to 7 reprocessing cycles, using multiple injection molding with constant injection parameters, monitoring the evolution of rheological, thermal, and mechanical properties and reporting an increase of crystallinization and a severe depletion of the mechanical properties as a function of the processing cycles, explained by the strong degradation of the polymer during processing, which yields large chain scission evidenced by rheological experiments and molecular weight measurements [37]. Zenkiewicz *et al.* studied the rheological, thermal, and mechanical changes up to 10 reprocessing cycles using successive extrusion of PLA, and reported a depletion of mechanical properties, a slight decrease in thermal stability

and a significant increase in melt flow rate as a function of the extrusion number [38]. However, the author states that PLA regrind could be further used as an additive to the neat polymer [38]. Sanchez *et al.* analyzed the recyclability of PLA up to 5 reprocessing cycles using FFF technology and micro-injection molding for monitoring mechanical changes caused by degradation mechanisms occurred during the polymer recycling, reporting that it was feasible to use recycled PLA for open-source AM, although the decrease in the mechanical properties induced by the 3D printing manufacturing cycle indicate that the material cannot be recycled as many times as in the injection molding process [39].

2.2.3   Degradation mechanisms characterization

Throughout different experiments on PLA recyclability, the influence of degradation mechanisms on the structure, mechanical properties, and long-term stability of the recycled polymers is reported, thus highlighting the importance of extensive detailing the modifications undergone by reprocessed polymers on both molecular and macroscopic levels [2; 6]. Analysis of the alterations in chemical functional groups of the polymer via vibrational spectroscopy, determination of thermal properties, degree of crystallization, morphological modifications, monitoring the chemical composition and molecular weight distribution, as well as to monitor the mechanical properties, allow for an extensive characterization of the key factors that will affect the final properties of the recycled polymer. Altogether, this data enables to the tune the mechanical recycling parameters for achieving an extended life for these valuable resources [6].

Regarding the melt (re)processing of PLA, the main thermomechanical degradation pathways are related to the random chain scission and inter/intramolecular transesterification, which lead to the formation of low molecular weight compounds, such as linear hydroxyl, ester, and carbonyl groups, as well as lactide and cyclic oligomers, respectively [40; 41]. Moreover, external factors such as the presence of moisture, lactide acid residues, and metal catalysts favor the molecular degradation of the polymeric chains [42]. In this context, a degraded PLA is identified as a polymer with low molecular weight and high polydispersity index, which will influence its rheological, thermal, and mechanical properties [2; 43].

Mechanical properties

After thermomechanical recycling of PLA, the general trend is a slight decrease of its native mechanical properties, particularly tensile, flexural, and impact resistance, which can compromise its performance in second market applications [37]. Brüster *et al.* reported that the PLA tensile modulus does not significantly change as a function of the reprocessing cycles, whereas the strain at break markedly decreases [44]. In this scenario, the embrittlement of PLA is attributed to variations on its microstructure and molecular structure [44]. Pillin *et al.* reported similar results and demonstrated that the steadiness of tensile modulus resulted from the synergetic effect between the decrease in molecular weight and the increase in crystallinity, both consequences of the degradation induced by the mechanical recycling processes [37]. Additionally, low molecular weight compounds and increased crystallinity favor the crack propagation above the elastic domain, which explains the embrittlement of the material and the evident decrease in both ultimate

stress and strain at break [37].

Morphology

For assessing the microstructure of the reprocessed polymer, powerful microscopic techniques, such as scanning electron microscopy (SEM) and transmission electron microscopy (TEM) can be employed [6]. Agüero *et al.* reported that after two reprocessing cycles more marked crack fronts were observed on the PLA-based samples, and that this new morphology was responsible for the embrittlement of the material, resulting in a less energy absorption during impact conditions [45]. The degradation of the material was also identified by optical measurements, which demonstrated a yellowish coloration experienced by the PLA pieces with the increased number of reprocessing cycles, a behavior that is linked to the molecular weight reduction and the presence of chromophore groups [42; 45].

Crystallinity and thermal properties

Changes on the polymer's physical properties such as crystallinity, melting behavior, and thermal history, can also be used as indicator of the degradation degree and the quality of recycled plastics [6]. Thermal analysis techniques such as differential scanning calorimetry (DSC) are widely used for these purposes [6].

Several authors report that the successive reprocessing cycles do not influence the glass transition temperature (T_g) of PLA [42; 44; 46]. However, Badia *et al.*, Cuadri *et al.* and Pillin *et al.* reported a slight decrease in its T_g after multiple extrusion or injection molding cycles, whereas Agüero *et al.* reported an increased T_g after three reprocessing cycles, with both behaviors being attributed to the modification of molecular weight and molecular weight distribution within the polymeric chains [37; 40; 43; 45].

Regarding the melting behavior of the recycled polymers, Zenkiewicz *et al.* and Pillin *et al.* reported a decrease in the PLA melting temperature (T_m) as a function of the number of processing cycles [37; 38]. Additionally, the presence of a double melting peak was identified by several authors on recycled PLA and attributed to the melt recrystallization process caused by the coexistence of crystals with different extents of perfection that melt at equally different temperatures [40; 44; 46; 47].

Crystallization kinetics are also affected by mechanical recycling processes [46]. The crystallinity of pristine PLA has been described as a function of the ratio between the two dimer stereoisomers (L-lactic acid and D-lactic acid), where a PLA containing less than 7% D-lactic acid is considered semi-crystalline, while a PLA with more than 7% D-lactic acid is completely amorphous [8]. Several authors report that a higher mobility of the polymeric chains due to chain scission phenomena will favor the increase in crystallinity of reprocessed PLA [37; 44; 45; 46; 47; 48].

The cold crystallization is an exothermic crystallization process that results in the formation of small crystallites at relatively low temperature, above the glass transition temperature of the polymer. Beltrán *et al.*, Botta *et al.* and Zenkiewicz *et al.* report an evident decrease in the cold crystallization temperature (T_{cc}) after successive reprocessing of PLA [38; 46; 47].

Analysis of alterations in chemical functional groups

Fourier-transform infrared spectroscopy (FTIR) is a technique widely used to evaluate the conversion of functional groups in polymeric materials, allowing the quantification of various types of transformations within their chemical and physical structure [42]. For PLA, the main peaks in the FTIR spectra are related to the asymmetric and symmetric C-H stretching of the CH_3 group, which can be identified in the regions between 3100-2800 cm^{-1} and the CH_3 deformation vibration in the region between 1470-1450 cm^{-1} [7; 41; 44]. Moreover, asymmetric and symmetric vibration of the ester group of PLA can be identified in the region between 1220-1085 cm^{-1}, whereas carbonyl groups (-C=O) are located in the region around 1800 cm^{-1} to 1700 cm^{-1} [7; 40].

Bands in 1293-1207 cm^{-1} (due to alkyl-ketone chain vibrations) and 920 cm^{-1} (due to flexural C-H bond vibration) are representative of crystalline structures in PLA [40; 42; 43]. The appearance of carbonyl-linked species has been reported as a symptom of molar mass reduction due to polymer degradation [6; 43]. However, several authors documented the inexistence of additional functional groups, particularly end-groups, in recycled PLA when compared with non-recycled PLA [43; 44]. This limited structural transformation suggests that the main thermomechanical degradation mechanism is related to random chain scission phenomena [44; 47].

Molecular weight distribution and composition

The main degradation pathways for PLA result in a loss of molecular weight and dispersion of molecular weight distribution due to the cleavage of the polymeric chains and their subsequent higher mobility during melt processing and mechanical recycling [44]. In this context, it is crucial to monitor the evolution of molecular weight and polydispersity index in reprocessed polymers, which can be obtained directly by employing a size exclusion chromatography (SEC) technique or indirectly by assessing the rheological behavior of the polymeric material [6].

In general, it is difficult to achieve very high molecular weight for biopolymers due to synthetization constrains, which is unfavorable for their recyclability [49]. From the scientific literature, 132.000 g/mol has been postulated as the critical molecular weight for PLA, and different authors have reported a significant decrease in its weight average molecular weight (M_w) as a function of reprocessing cycles [44]. In particular, Scaffaro *et al.* has reported a decrease in the PLA's M_w between 4% and 8% after a single extrusion cycle, whereas Botta *et al.* has reported a M_w decrease of 22% after five reprocessing cycles [46; 50]. A more drastic decrease was identified by Pillin *et al.*, which reported a 50% M_w decrease after three injection molding cycles [37]. An increase in polydispersity index, which is a parameter related to the molecular weight distribution and, particularly, to the presence of a certain fraction of small, volatile molecules, is also reported and attributed to thermomechanical reprocessing [42].

The rheological properties of PLA are also affected by the its molecular degradation since they are related to the melt viscosity and, therefore, to the molecular weight of the polymer [6]. Melt flow rate (MFR) represents a useful parameter to estimate the processability of materials, particularly for polymers that have a high tendency for thermo-hydrolytic degradation, such as PLA [51]. Moreover, MFR is a simple test that requires low-cost equipment and can potentially provide information about degradation

in a polymeric material, although not as detailed as other more powerful techniques, such as oscillatory rheometry, which accounts for the variation of temperature and shear rate [45]. A progressive increase in the MFR has been extensively reported as a consequence of consecutive processing steps [38; 39].

The molecular weight decrease in recycled PLA is undesirable not only because of the minimized material melt strength and mechanical properties, but also because the processing equipment can be damaged due to the volatile lactic acid formation, thus enhancing the importance of designing strategies for its recovering in order to achieve a reliable recycling-based valorization pathway [5; 40].

2.3   Reprocessing Plastics: Upgrading strategies

Different strategies including restabilization, rebuilding of the polymeric chains, compatibilization with other polymers, incorporation of a certain percentage of virgin material together with the recycled polymers, the addition of elastomers/fillers, and thermal treatments, such as annealing, can be employed to upgrade the structure and performance of recycled PLA [2].

Before processing, polymers are usually blended with different kind of additives in order to improve mechanical/thermal/rheological properties, widen their processing window and prevent degradation [6]. However, when handling recycled polymers most of these components have already been consumed during processing and service-life and, therefore, must be readded during the mechanical recycling processes [6]. The addition of stabilizers [2; 37], impact modifiers [50] and nucleation agents to control crystallinity [52] are common approaches reported in the literature for PLA restabilization.

Apart from the restabilization strategies, the rebuilding of the degraded polymeric chains through the application of reactive additives, such as chain extenders, has been a subject of extensive research [2]. Chain extenders (CE) are able to reconnect the cleaved chains, thus allowing molecular weight restoration, as well as the improvement of mechanical and thermal properties of the recycled materials [7; 53]. Furthermore, according to the CE's functionality, variations on the polymer structure, in particular, the formation of long branched chains can contribute to improve the polymer's melt strength [49; 54].

The functionality of a CE is attributed to the number of reactive sites available on its structure. In this context, a di-functional CE with two reactive sites will couple exactly two, typically equal, end-groups, in order to form a strictly linear polymer chain [49; 55], whereas a multifunctional CE with more than two functional groups will result in branched or cross-linked structures [56]. However, a relatively high amount of linear chain extender is required to get a significant increase on the molecular weight, whilst overdosing the material with a multifunctional CE can lead to overcrosslinking and gelation, making the polymer impossible to be processed with regular extrusion or injection molding equipment [49].

For PLA, the incorporation of functional CE will favor the reaction with carboxyl and hydroxyl groups and can be either applied directly through reactive extrusion or by employing an additional melt-mixing stage [57; 58]. Several authors have addressed the possibility of rebuilding degraded PLA through multifunctional chain extenders, particularly epoxy-based CEs, such as Joncryl ADR 4368, reporting improvements on the material's molecular weight and molecular weight distribution without sacrificing its mechanical and thermal performance [7]. Meng *et al.* studied the influence of phosphite-based CEs on the performance of PLA, reporting a significant improvement of toughening properties [59; 60], whereas Han *et al.* addressed the possibility of using functional polysilsesquioxane (FPSQ), which has no detrimental influence on the environmentally friendly properties of PLA and allows for effective chain extension, enhancing its melt rheological properties [61]. Herrera *et al.* studied the effect of incorporating different CEs in distinct polymerization stages, particularly 1,3-phenylene-bis-2-oxazoline (PBO) and 1,10-carbonyl bis caprolactam (CBC), concluding that PLA-CE systems were less sensitive to degradation than the neat PLA [53].

While the molecular weight restoration is the most obvious effect of chain extension on recycled polymers, other properties will also be affected. Alturkestany *et al.*, Julien *et al.* and Rasselet *et al.* reported no significant change in thermal transition temperatures of PLA after its chain extension [55; 62; 63]. However, Khankrua *et al.* reported a slight increase on both melting temperature (T_m) and glass transition temperature (T_g) while the CE content increased [7], whereas Barletta *et al.* reported a slight decrease of the melting temperature (T_m) attributed to the resulting branched structure [51]. Crystallization kinetics will also be affected by the chain extension reactions since the increased molecular weight is related to a higher restriction of chain mobility which is unfavorable for the formation of crystals within the polymeric matrix [56]. Additionally, cold crystallization temperature (T_{cc}) is also affected by the CE incorporation. Najafi *et al.* and Rasselet *et al.* reported an increase in T_{cc} while increasing the CE content [56; 62], whereas Barletta *et al.* reported a decreasing of T_{cc} due to the presence of Joncryl ADR 4368 chain extender, which can act as a nucleating agent [51].

Regarding the mechanical performance of PLA after chain extension, Barletta *et al.* and Rasselet *et al.* reported a significant increase in tensile properties, reflected by an enhancement of ultimate stress and elongation at break [51; 62]. Moreover, Alturkestany *et al.* reported that the increased branching resulting from the increasing CE content had a correspondent benefit on tensile strength, which increased [63], and Tuna *et al.* highlighted a shift from a brittle to ductile behavior on fracture [57]. Liu *et al.* report an increase in melt viscosity [8], which is also presented on the studies by Ghalia *et al.* and Baimark *et al.* that highlight a significant decrease in MFR after complete reaction of PLA with the chain extender [54; 64]. The ideal CE content seems to be highly dependent on both the polymer's degradation degree and the processing conditions, since more degradation of the polymer chains will lead to more active sites available to react with the CE, but unreacted chain extender dispersed within the polymeric matrix will have an undesirable effect on the rheological properties [7; 62]. Furthermore, there are concerns about the effect of the incorporation of CE on the PLA compostability, since the presence of additives of any kind in PLA at concentrations above 1 wt% may affect its compostability certification [56].

In general, rebuilding degraded polymer chains through chain extension will favor the formulation of a polymer with restored molecular weight and stable properties that can possibly fulfill the rheological requirements of a wide range of polymer processing techniques [8], including additive manufacturing technologies, such as FFF [63; 65].

2.4   Challenges for a closed-loop recycling using FFF

Within the circular economy concept, closed-loop recycling stands for a recycling system where the waste materials are used to produce the same products that they were originally recovered from [5]. In this context, for a FFF manufacturing cycle, waste can be derived from scrap components, such as bed adhesion and overhang supports and failed parts that do not fit the quality control standards, as well as discarded parts from consumers and consumers-manufacturers that can be collected based on the extended producer responsibility (EPR) or distributed recycling via additive manufacturing waste management (DRAM) strategies [17].

However, there are several limitations related to waste-to-product valorization pathway using extrusion-based AM technologies such as FFF, regarding the material behavior, upgrading strategies, and, particularly, the inherent processing stages [66]. To properly recycle a product through FFF manufacturing technology, conventional mechanical recycling processes such as size reduction, drying, and extrusion have to be employed in order to obtain a high-quality monofilament to be further used in 3D printing applications [39].

For the drying stage of PLA-based materials, different approaches are found in the literature with temperatures ranging between 50 °C and 110 °C and drying periods between 2h and 24h. The main purpose of the drying stage is to limit the absorbed moisture as much as possible in order to inhibit hydrolysis reactions during the melt processing. In this context, a moisture content below 0.5% or achieving constant weight are commonly accepted criteria [50; 66].

Further, the filament extrusion stage is fundamental for the success of the closed-loop recycling cycle. Different equipment provide equally different extents of control over the process, particularly the thermal stages number, type of cooling, screw speed, and puller system velocity, which shall be tuned according to the material behavior and will determine the physical properties of the monofilament, such as the filament diameter and cross-sectional shape. Filament diameter tolerance is considered as an important indicator of 3D printing quality by commercial filament suppliers, 3D printer manufacturers, and consumers, since irregular filament diameter can negatively affect the flow rate during extrusion which can cause a variety of problems including poor surface quality, extruder jams, voids, or excessive overlap, and eventually lead to failed or rejected builds [67].

Many FFF printers have very low tolerance for filament diameter variation. A filament which is too large can get stuck at the extruder, whereas a filament with an unexpected small diameter can cause the mechanism to not being able to grip the filament due to a lack of tension [66; 68]. A solution for obtaining filament of uniform diameter is to use an automatic puller speed control based on in-line diameter measurements. However, the success of this approach is dependent on the remaining process parameters and hardware setup and will be more challenging as the material is further reprocessed due to the melt viscosity lowering [68]. On the other hand, when handling mixtures between the virgin or recycled polymer and a CE, another set of problems is expected since the increased molecular weight is related to an increase in melt viscosity, which in turn raises the pressure provoked in the equipment [58]. In this context, decreasing the screw speed and increasing the thermal stages temperature starting from the die to the

feeding zone is considered a standard procedure [58].

Apart from filament diameter tolerance considerations, the winding procedure is also an important constrain for the production of high-quality 3D printing filament. After extrusion 3D printing feedstock is generally winded up in spools which can then be placed on the FFF machine for continuous material feeding. However, unproper winding can lead to the filament entanglement within itself and break down during the printing, resulting in failed 3D parts. Although there is not a general solution for filament entanglements, controlling the tension between the puller system and the winder help to minimize this problem.

Regarding the 3D printing of recycled materials, material behavior characterization during the melt processing is of uttermost importance since this technology is highly dependent on thermodynamic and rheological considerations, such as the non-Newtonian fluid heat transfer, extrusion behavior, and molecular diffusion which allows for both deposition and bond between strings and layers [64].

Generally, the FFF machine apparatus resembles the first injection molding machines, where the filament has a double functionality: to act as a piston and to generate pressure on the hot end, but also to supply the feedstock for the conformation of the 3D part as it melts [69]. In this context, 3D printing filament is required to be flexible while solid, so it can be continuously pushed towards the hot end and provide enough pressure, but sufficiently strong in the molten state to allow for a controlled extrusion. In fact, FFF machines can only adopt materials which have viscosity in a limited range, as the viscosity should be high enough to provide structural support and low enough to enable extrusion [70]. Several authors address quality control parameters, such as MFR to categorize the material's printability [38; 42; 45]. Although MFR does not represent a fundamental polymer property, it is critically influenced by its physical properties, molecular structure and conditions of measurement, particularly temperature and applied load [71]. Typically, PLA with a MFR below 10 g/10 min (measured at 190°C with 2.16 kg load) is considered printable [66].

Throughout the literature review, the principles and specifications of the FFF technology from the production of monofilament to the production of value-added 3D parts were addressed. Moreover, the framework of the research question regarding the incorporation of recycled polymers and, particularly, recycled PLA into sustainable value chains is highlighted and the challenges and opportunities for developing a closed-loop recycling scheme involving recycled-recovered PLA were postulated according to the state-of-art literature.

In the following chapter, the experimental methodology involving a multi-processing approach in order to address the recyclability of PLA and to set a path for achieving a circular value chain based on additive manufacturing applications, particularly Material Extrusion or Fused Filament Fabrication is described. To accomplish these objectives, the general processes for the production of 3D printing feedstock, including material preparation and filament extrusion, as well as the production of 3D parts and subsequent recycling were simulated at laboratorial scale. Moreover, analytical methods were employed in order to characterize the evolution of the material's properties from different perspectives and to quantify the influence of degradation mechanisms due to processing and mechanical recycling. Further, a functional additive, PBO, that which can act as a

chain extender, was incorporated into the polymer in order to understand to which extent the recovery of the degraded polymeric chains caused by the chain scission phenomena could help to upgrade recycled PLA to be further integrated in a closed-loop recycling scheme.

Part III

Experimental work

Chapter 3

Experimental work

After gathering the required knowledge about additive manufacturing, plastic recycling, and upgrading strategies, an experimental procedure was implemented in order to understand the possibility of establishing a closed-loop recycling scheme for PLA and involving extrusion-based AM technologies. Furthermore, a fixed amount of a CE was incorporated into the neat and recycled polymer to address the hypothesis of property recovery of the PLA/CE systems. In this context, this chapter aims to present the material and methods implemented through the experimental component of this study by focusing on the fabrication of samples, processing equipment, and evaluation of properties.

3.1   Materials and methods

An industrial-grade PLA, ErcrosBio® LL 602, produced by Ercros (Spain) and supplied by AGI (Vila Nova de Gaia, Portugal) was selected for addressing an FFF-based multi-processing approach. According to the manufacturer's specifications, this grade of PLA is primarily intended for injection molding applications. From its technical data sheet (TDS), it is known that the material has a density of 1,25 g/cm³, tensile modulus of 3000 MPa, tensile strength of 68 MPa, tensile elongation of 3%, a glass transition temperature of 63 °C and MFI of 17 g/10 min, measured at 195 °C and 2,16 kg load. Prior to processing the material was dried in a convection oven at 60 °C for 9 h in order to stabilize its moisture content. 1,3-Bis(4,5-dihydro-2-oxazolyl)benzene (PBO), supplied by TCI Chemicals (Zwijndrecht, Belgium) was used as chain extender for virgin and recycled PLA. This component has a weight-average molecular weight of 216.24 g/mol, melting temperature between 146 °C to 149 °C and is provided in powder.

Four different recycling chains, presented in Table 3.1 and composed by the processes of material preparation, extrusion of filament, fabrication of samples, evaluation of properties and plastic recycling were employed in order to access the recyclability of PLA and the recovery of its properties via the addition of a functional chain extender, following a methodology adapted from the work by Sanchez *et al* [39]. The first recycling process chain was based on neat PLA and will be referred hereafter as vPLA. A second recycling chain based on recycled PLA obtained through a mechanical recycling simulation encompassed by the processes of drying, extrusion of filament and 3D printing was considered as a reference for the behavior of the recycled material and will be designated hereafter as rPLA. The remaining recycling process chains were obtained by the compatibilization

Table 3.1: Description of the four different recycling chains, the processing steps, and characterization methods followed (Adapted from [39]).

Recycling Chains	Material Preparation		Granules			Processing		Plastic Recycling
vPLA	Drying	Melt mixing	Virgin PLA	FTIR, DSC and MFI samples preparation		Extrusion of Filament	3D Printing	Plastic Shredding
rPLA	Drying		Recycled PLA	FTIR, DSC and MFI samples preparation		Extrusion of Filament		
vPLA+PBO	Drying	Melt mixing	Virgin PLA	PBO 1% w/w	FTIR, DSC and MFI samples preparation	Extrusion of Filament	3D Printing	Plastic Shredding
rPLA+PBO	Drying	Melt mixing	Recycled PLA	PBO 1% w/w	FTIR, DSC and MFI samples preparation	Extrusion of Filament	3D Printing	Plastic Shredding

of the neat and recycled polymer with the CE and will be referred as vPLA+PBO and rPLA+PBO, respectively. The CE content was fixed on 1% w/w based on the knowledge gathered from previous works involving the upgrading strategies for recycled PLA [53].

3.1.1   Fabrication of samples

To establish the influence of material degradation on the PLA and PLA/PBO systems, different tests including the monitoring of alterations on the polymer structure, processability, and evaluation of thermal and mechanical properties were conducted. In this context, different samples were recovered from different stages of each manufacturing chain.

From the PLA-based pellets, a certain quantity of material was reserved for the DSC ($\approx$0,2 g), MFI ($\approx$30 g) and FTIR ($\approx$4 g) analysis. Particularly, the vibrational spectroscopy analysis required the conformation of thin flat film which was obtained by means of a hot plate press at the temperature of 200°C and a pressure around 100 bar for 1 min. These films were also used for employing a color measurement analysis based on the CIElab color profile. The DSC and MFI samples preparation was conducted according to the compliant standards (ISO 11357 and ISO 1133, respectively).

Further, random segments of PLA-based filaments were selected for accessing the material mechanical behavior following the standard test for determining the tensile properties of single-filament materials (ASTM D3379). In this context, a cardboard mounting tab similar to the one presented in Figure 3.1 was developed in order to decrease the clamping breaks which lead to the failure of the test. The filament test specimens have a gage length of 60 mm and were fixed to the mounting tab by means of a hot glue bead. Moreover, small segments of filament were broken after being exposed to -70 °C for $\approx$15 min in order to obtain a clean cross-section for the SEM analysis.

The remaining samples were produced through the FFF technology, particularly a regular dodecahedron for performing a 'printability' test and dumbbell-shaped test specimens (ISO 527-02, Type 1BA) for accessing the tensile properties of the material after being processed though the FFF technology. Both models were developed through the educational version of SOLIWORKS 2020 CAD software, converted to a STL file and pre-processed with ULTIMAKER CURA 4.9.1 slicing software, using the process
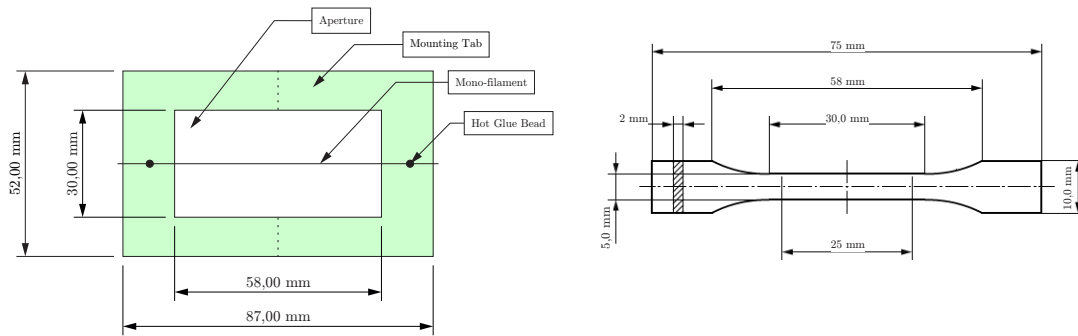
Figure 3.1: Representation of the mounting tab for single-filament tensile tests (Adapted from [72] - left) and technical specifications for the ISO 527-02 Type 1BA dumbbell tensile test specimen (Adapted from [73] - right)

parameters further described in the context of this document.

Over the course of this study, it was of uttermost importance to decide which equipment and processing conditions were most suitable for employing the proposed methodology, particularly regarding the stages of material preparation, extrusion of monofilament and fabrication of samples through the FFF technology. In this context, this section is dedicated to exploring, within the available equipment, which ones were more suitable for employing a multi-processing approach of PLA for AM applications and aims to provide knowledge for future studies and establish procedures that can be employed either on a laboratory or industrial scale.

Extrusion of monofilament

Regarding the extrusion of monofilament stage, two different single-screw desktop filament extruders were available, particularly a NOZTEK PRO FILAMENT EXTRUDER (Noztek, UK)[1] and a NEXT 1.0 ADVANCED (3devo, Netherlands)[2]. The NOZTEK PRO FILAMENT EXTRUDER (Figure 3.2 - left) is equipped with a screw and barrel unit with a L/D (length/diameter) ratio and screw diameter of 18.57:1 and 14 mm, respectively. It provides one temperature control band and has a fixed screw speed which guarantees 2.5 m/min extrusion rate according to the manufacturers specifications, as well as a single cooling fan system displaced right after the 1.75 mm cone-shaped brass nozzle. With the available set-up for this equipment, the conveyor system was composed of a steel sheet and the puller speed control and winding procedures were performed manually. Moreover, the 45° placement of the equipment represents an important feature for processing pellets, powder or flakes since it facilitates the feeding operation by ensuring that the material does not get stuck on the hopper walls.

Several experiments were conducted using this equipment based on either virgin or recycled PLA-based materials with a temperature profile ranging between 120 °C and 190 °C. However, the manual puller speed control and inefficient cooling led to a brittle filament with an inconsistent diameter which presented occasional creases due to the lack of a winding system. In this context, only small segments about one meter long were

---

[1]Universidade de Aveiro - Departamento de Engenharia Mecânica, Aveiro
[2]Universidade de Aveiro - Departamento de Materiais e Cerâmica, Aveiro

able to be produced, which caused a constraint to further processing and excessive waste of material.

On the other hand, 3devo's NEXT 1.0 ADVANCED (Figure 3.2 - right) is an all-in-one bundle, which includes an extruder equipped with a nitride hardened steel extruder screw, four independent heating bands, a precise screw speed control, a cooling unit composed of a double fan and an automated puller speed control, positioner and winding system based on in-line diameter measurement through an optical sensor which allow enhanced reliability and repeatability for the production of high-quality feedstock for FFF applications. In this scenario, the 3devo's NEXT 1.0 ADVANCED represents a solution which provides a greater extent of control over the process and an easier-to-upscale procedure, since it resembles a typical industrial extruder line for the production of 3D printing filament and, therefore, was the equipment of choice to be employed on the context of this work.

By using this extruder, the challenges of dynamic puller speed control and proper winding were surpassed, and the diameter consistency could be monitored via the equipment's USB-connectivity which allowed to plot the filament diameter, as measured through the optical sensor, against time. The average extrusion rate achieved was around 2 m/min and the material loss factor due to the extrusion process was always less than 20%. The main limitations associated to this equipment are related to the single stage air cooling which contributes to the brittle behavior of the filament and the feeding system design which is not suitable for processing flakes, regrinds or powders, since these materials have a rough structure and tend to form cohesive structures inside the hopper which prevent a stable feeding of material into the extruder.

FFF machines

Three different cartesian FFF machines were considered during the course of this study, particularly a HELLO BEE PRUSA (BEEVERYCREATIVE, Portugal)[2], a B2X300 (BEEVERYCREATIVE, Portugal)[1], and a ENDER 3 (Creality, China). From these, and since the diameter consistency was always a major concern on the custom PLA-based formulations, the direct drive extruder-based HELLO BEE PRUSA (Figure 3.3 - left) was theoretically the most suitable option as this type of equipment has typically a broader tolerance for diameter deviations. However, due to the smooth surface and brittle behavior of the PLA, the equipment was not able to correctly grip the filament, which was prone to get stuck in the interface between the cold and the hot end. In this context, the Bowden extruder-based B2X300 (Figure 3.3 - center) 3D printer was considered since it features a more powerful extruder unit and an all-metal hot end which has been proved to provide enhanced efficiency. Although a higher success rate was achieved while using this alternative equipment, the long distance between the cold end extruder and the hot end provided too much space for the brittle filament to break, so an intensified attention by the operator was required in order to achieve a successful print.

In order to overcome this challenge, a set of experiments were conducted on a Bowden extruder-based ENDER 3 (Figure 3.3 - right) which guarantees a smaller distance between the cold end and the hot end by placing the cold end extruder unit in the Z axis.

---

[1]Universidade de Aveiro - Departamento de Engenharia Mecânica, Aveiro
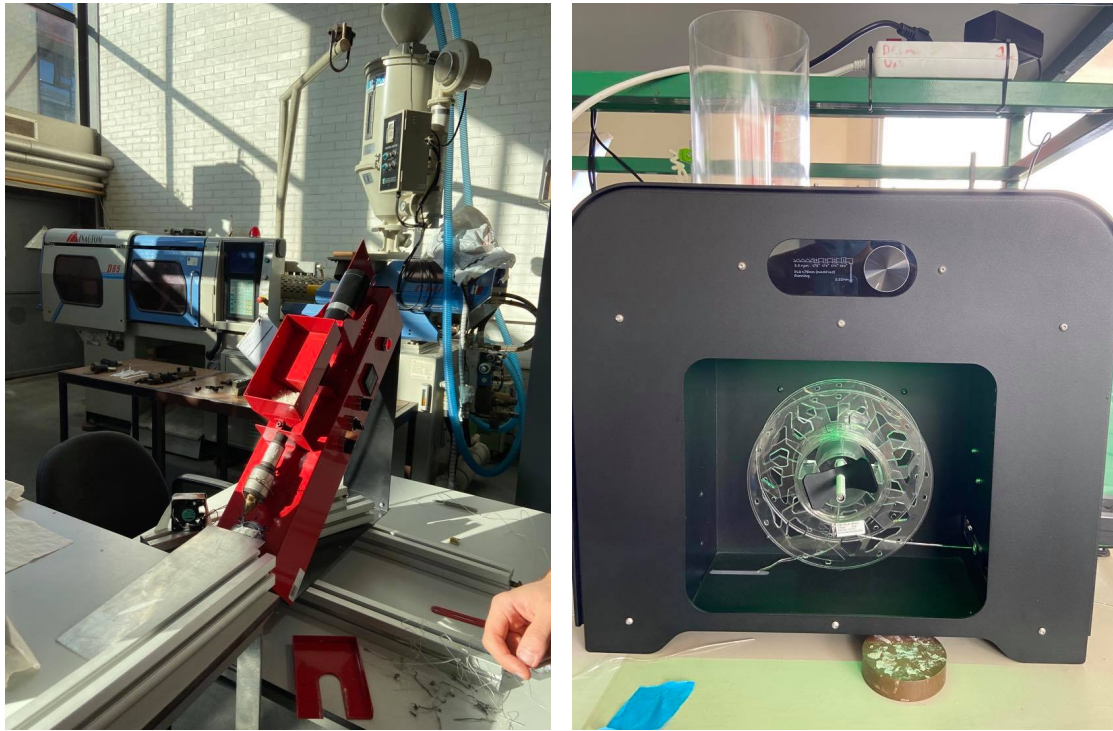
Figure 3.2: Representation of the equipment used in the context of the extrusion of monofilament stage NOZTEK PRO FILAMENT EXTRUDER (left), 3DEVO NEXT 1.0 ADVANCED (right).

Since all the machines employed could achieve the selected process parameters, they were kept constants for all the experiments.

3.1.2 Processing equipment

In order to obtain a homogenous mixture between the PLA and the chain extender, a laboratory-scale mechanical melt-mixing process was employed by using a PLASTOGRAPH EC BRABENDER (Brabender GmbH Co. KG, Germany)[3] torque rheometer. For each batch 250 g of PLA were considered, and for the compatibilized formulations 2.5 g of PBO were added after the complete melting of the polymer in order to fulfill the desired CE concentration. The mixing conditions were set according to the material melt behavior. In this context, the equipment temperature was set up to 180 ℃, the speed to 75 rpm and the residence time from 5 to 10 min. After the blending stage, the obtained mixtures were grinded to ≈2 mm flakes which allows it to be fed to the filament extruder.

The extrusion of monofilament was conducted on a NEXT 1.0 ADVANCED (3devo, Netherlands)[2] desktop filament extruder, equipped with an in-line diameter sensor and an automated winding system. The temperature profile employed, from the die to the feeding zone was 180 ℃, 175 ℃, 170 ℃, 165 ℃ and the screw speed was set

---

[3]ESAN - Oficina de processos industriais, Oliveira de Azeméis
[2]Universidade de Aveiro - Departamento de Materiais e Cerâmica, Aveiro
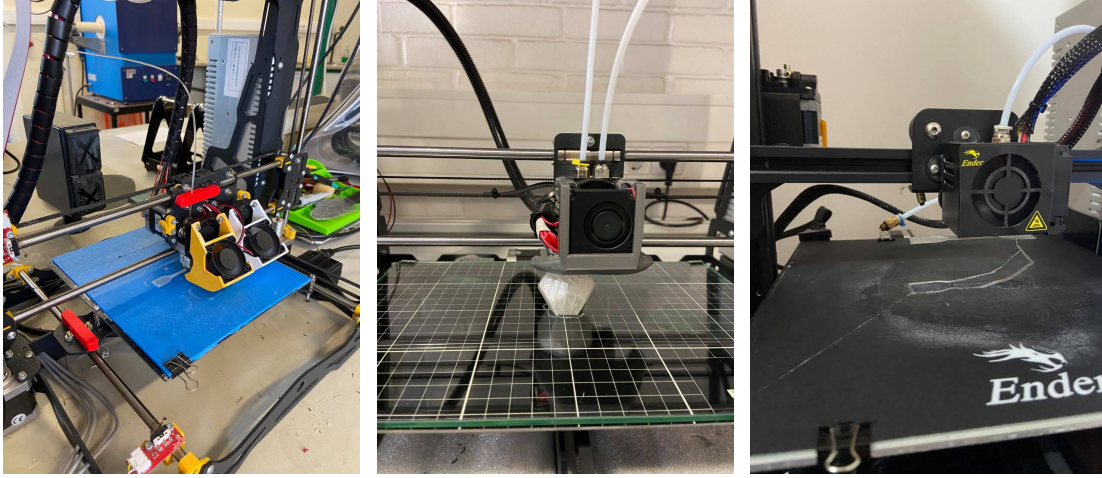
Figure 3.3: Representation of the equipment used in the context of the 3D printing stage: HELLO BEE PRUSA (left), B2X300 (center) and ENDER 3 (right).

up to 4 rpm. The success criteria for the production of monofilament was the diameter consistency which was set within a range between 1.65 mm and 1.85 mm, with 1.75 mm as the diameter sensor target.

The selected FFF machine was a ENDER 3 (Creality, China), an open-source cartesian 3D printer, equipped with a Bowden tube-based extruder and which has been the equipment of choice for many hobbyists and consumer-manufacturers since it represents a low initial investment and has a large online support community. Prior to the machine operation, a G-code which includes the process parameters and coordinates of the part was generated with the aid of the slicing software ULTIMAKER CURA 4.9.1. The process parameters, which were crafted according to the part specifications and material melt behavior, are presented in Table 3.2. For the 3D printing stage, the success criteria employed was the correct fabrication of the part without any major defects which could be detected by a visual inspection, as well as its correct extraction from the printing platform. As a post-processing procedure the removal of the bed adhesion supports such as the brim or skirt were conducted to all the parts produced through the FFF machine.

The size reduction stage of PLA-based 3D printed parts was conducted on a WANNER C 13.20S plastic granulator (Wanner Technik GmbH, Germany)[2] equipped with a 2 mm sieving unit. According to the manufacturer, this equipment was designed in order to reduce friction on the cutting chamber, preventing the warming up of the blades and, therefore, limiting the rate of thermo-mechanical degradation on the regrind [74].

3.1.3   Characterization of the PLA- and PLA/CE-based materials

Production of filament

The linear mass density (μ) of the filament was calculated from the ratio between the filament weight and the filament length by following Equation 3.1. The theoretical linear mass density (μ_t) was determined through the polymer's density as stated in the

Table 3.2: Processing parameters used for the fabrication of the 3D printed samples (Adapted from [39])

	Dumbbell (ISO 527-02, Type 1BA)	Regular dodecahedron
Toolpaths	90°-90°	90°-0°
Layer height	0.1 mm	0.2 mm
Bed temperature	60°C	60°C
Extruder temperature	190°C	190°C
Wall line count	2	2
Top layers	4	4
Bottom layers	4	4
Infill density	100%	15%
Travel speed	150 mm/s	200 mm/s
Nozzle diameter	0.4 mm	0.4 mm
Raster width	0.5 mm	0.48 mm
Print speed	40 mm/s	80 mm/s
G-code	Ultimaker Cura 4.9.1	Ultimaker Cura 4.9.1

manufacturer TDS and the filament average cross-sectional area as seen in Equation 3.2.

$$\mu = \frac{Filament\ weight}{Filament\ length}\ [g/m] \tag{3.1}$$

where μ represents the linear mass density in g/m. The filament weight (g) was measured after extrusion on an analytical balance, and the filament length (m) was obtained through the extruder's data acquisition software.

$$\mu_t = d \cdot A_c\ [g/m] \tag{3.2}$$

where μ_t represents the theoretical linear mass density in g/m, d the density in g/cm^3 and A_c the filament cross-sectional area in mm^2.

Moreover, and, since the process parameters for the extrusion stage were kept constants for all formulations, the evolution of the extrusion rate was calculated by following Equation 3.3.

$$Extrusion\ rate = \frac{Filament\ length}{Extrusion\ time}\ [m/min] \tag{3.3}$$

where *Filament length* (m) and *Extrusion time* (min) were obtained through the extruder's data acquisition software.

Tensile tests

Tensile tests of the filaments were achieved by means of a TA.XT PLUS C texture analyzer (Stable Micro Systems, UK)[4] equipped with a micro tensile grip. For all the samples, the selected loading speed was 1 mm/s and a 300 kN load cell was used.

---

[4]Universidade de Aveiro - CICECO, Aveiro

Moreover, tensile tests of the specimens produced through FFF technology were conducted on a universal tensile testing machine AUTOGRAPH AGS-X SERIES (Shimadzu, Japan)[1]. At least four replicates were tested, at a loading speed of 1 mm/min and a 50 kN load cell was employed.

Surface Morphology

Samples of all the formulations were analyzed on their cross-section. The images were collected using a scanning electron microscope (Hitachi TM4000Plus, Japan)[5], operated at 10 kV. Carbon conductive tape was applied to the sample holder before analysis to avoid charging. The images were recorded in the magnification range of x500 to x1000 at different locations on the surface.

Color Measurements

The chromatic properties were evaluated using a portable colorimeter CHROMA METER CR-400 (Konica Minolta Sensing, Inc, Japan)[2], calibrated with a white standard tile. The color coordinates L^*, a^*, and b^* were collected, where L^* stands for the luminance or the prevalence between black and white, a^* indicates the change from green to red, and b^* represents the change between blue and yellow [45; 75]. At least five replicates were obtained for each sample and the corresponding average values and standard deviations were calculated. The total difference in color (ΔE^*_{ab}) was calculated according to Equation 3.4.

$$\Delta E^*_{ab} = \sqrt{(\Delta L^*)^2 + (\Delta a^*)^2 + (\Delta b^*)^2} \tag{3.4}$$

where, ΔL^*, Δa^*, and Δb^* are the L^*, a^*, and b^* differences between each sample and the vPLA [75].

The color change was reported by addressing the following criteria: unnoticeable difference ($\Delta E^*_{ab} < 1$), slight difference ($1 \leq \Delta E^*_{ab} < 2$), noticeable difference ($2 \leq \Delta E^*_{ab} < 3,5$), evident difference ($3,5 \leq \Delta E^*_{ab} < 5$), and different colors ($\Delta E^*_{ab} \geq 5$) [45].

The yellowness index was obtained from the CIE color space values and the ASTM E313 method by considering an iluminant D65 and a standard observer function of 10°, following the Equation 3.5 [45].

$$YI = \frac{100(1.3013X - 1.1498Z)}{Y} \tag{3.5}$$

Differential scanning calorimetry (DSC)

DSC tests were conducted on a NEXTA STA300 heat-flux calorimeter (Hitachi, Japan)[2] using Linseis TA Evaluation software for data collection and treatment. Samples

---

[1]Universidade de Aveiro - Departamento de Engenharia Mecânica, Aveiro
[5]Universidade de Aveiro - TEMA, Aveiro
[2]Universidade de Aveiro - Departamento de Materiais e Cerâmica, Aveiro
[2]Universidade de Aveiro - Departamento de Materiais e Cerâmica, Aveiro

with weight between 5 mg to 10 mg were sealed in aluminum pans according to the sample preparation procedure described by the ISO 11357-1 standard. The samples were subjected to two heating steps, with the first heating schedule starting from 25°C to 120°C and kept at 120°C for 10 min. The second heating schedule started from 30°C to 250°C. An intermediate cooling step was also employed, starting from 120°C to 30°C and including a 10 min standby. All of the heating and cooling steps were conducted at a rate of 10°C/min and at least two replicates were scanned.

The main objective of the first heating scan was to eliminate the heat history of the samples, therefore, all the transition temperatures including the cold crystallization temperature (T_{cc}) and melting temperature (T_m), as well as cold crystallization (ΔH_{cc}) and melting (ΔH_m) enthalpies were recorded from the second heating sequence according to the procedures highlighted in the ISO 11357 standard.

Moreover, the melting enthalpy is known to be directly proportional to the crystallinity of a polymer. Therefore, the crystallinity ratio or degree of crystallinity (χ) can be determined by following Equation 3.6.

$$\chi(\%) = \frac{\Delta H_m - \Delta H_{cc}}{\Delta H_\infty} \qquad (3.6)$$

where ΔH_m and ΔH_{cc} (J/g of polymer) are the melting enthalpy and the cold crystallization enthalpy, respectively. ΔH_∞ is 93.1 J/g, which is the melting enthalpy for a 100% crystalline PLA [47].

FTIR spectroscopy

Infrared spectra of the samples were obtained with a Bruker compact FTIR spectrometer, model ALPHA (Bruker Corporation, USA)[6], using a PLATINUM attenuated total reflection (ATR) module on absorbance mode. First, a background spectrum was recorded and subtracted from the sample spectra in the area from 4000 cm^{-1} to 600 cm^{-1}. The number of scans was 32, with a wavelength resolution of 4 cm^{-1}. In order to assure accurate results, at least five replicates were conducted for each sample. Data collection was performed on the equipment's proprietary software OPUS 7.0 and exported to a custom excel datasheet.

Melt flow rate (MFR)

The measure of the MFR was conducted through a semi-automatic melt flow indexer MI-3 (Göttfert, Germany)[1], which determines the melt flow rate based on ISO 1133 Procedure A test standard. Following the manufacturer specifications test conditions (195 °C/2.16 kg), the polymer presented such a high fluidity that the test was impossible to conduct. In this context, several conditions were tested with temperatures ranging from 190 °C to 170 °C and a constant load of 2.16 kg. With the temperatures above 180 °C the fluidity was still too high for correctly employing the test procedure, however with temperatures below 180 °C the material did not completely melt, and the test results were discarded. The load was then reduced to 1.2 kg and the temperature set at 180 °C.

---

[6]Universidade de Aveiro - Complexo de Laboratórios Tecnológicos, Aveiro
[1]Universidade de Aveiro - Departamento de Engenharia Mecânica, Aveiro

At least three replicates were performed, each of those employing around 10 g of material through a Ø2.095 mm standard die.

Printability assessment

A qualitative approach for determining the 3D printing capacity of the material, either on its virgin, recycled, and compatibilized counterpart was conducted on the regular dodecahedron printed component, following an established criteria which includes the success of the print, and a visual inspection for defects such as the presence of voids, under or over-extrusion and layer shifts.

Throughout this chapter, the materials and methods that were employed during the experimental component of this research were presented, particularly the procedures implemented to the collection and fabrication of samples, including the processing equipment and parameters required, as well as the metrics for the evaluation of properties. In the following chapter, the obtained results are presented and discussed against the knowledge gathered from the literature review.

Part IV

Results and discussion

Chapter 4

Results and discussion

The following chapter presents the results obtained throughout the experimental work conducted over the course of this research and its discussion against the knowledge obtained from the literature review. In order to obtain a broader understanding regarding the polymer's property profile and processability, different metrics were monitored, including rates for filament production, mechanical behavior of both filament and printed specimens, surface morphology and optical measurements, structural and thermal analysis, MFR analysis and qualitative printability tests which were conducted to all the formulations of each recycling chain.

4.1 PLA-based Filament

From the results obtained from the analysis of the filament production rates, it can be highlighted that it was possible to extrude a filament with a consistent diameter, within the processable range for a general FFF machine, with all the formulations employed (Table 4.1). However, the high fluidity of the pristine PLA, the inefficient cooling of the filament extruder, and other hardware/software constrains, as stated in the experimentation stage of the experimental work, contributed for the production of a brittle filament, which undermined the further processing stages.

Moreover, from the analysis of the linear mass density consistency (Figure 4.1), it was possible to measure the presence of inclusions such as air bubbles or other contaminants trapped within the filament. In this context, vPLA presents a deviation between μ and μ_t of 31%. The remaining formulations, vPLA+PBO and rPLA+PBO, present a deviation between μ and μ_t of 12% and 14%, respectively. These results demonstrate that the virgin PLA was the most contaminated formulation, which may be related to the melt-mixing stage.

The quantity of filament produced, reflected by the output filament length indicates that this process does not represent an excessive waste of material, even when handling the 100% recycled polymer. For the filament produced with the rPLA the output filament length, extrusion rate and, consequently, the linear mass density were unable to be monitored due to an error in the data acquisition software. However, the filament average diameter was extrapolated from manual measurements and presented for sake of comparison. The evolution of the extrusion rate presents an increasing trend, particularly

Table 4.1: Characteristics of the filament produced with the different PLA formulations of each recycling chain.

	Average diameter (mm)	Filament Length (m)	Extrusion rate (m/min)
vPLA	1.764 ± 0.598	52.094	1.27
rPLA	1.702 ± 0.870 (*)	-	-
vPLA+PBO	1.722 ± 0.221	62.363	1.39
rPLA+PBO	1.740 ± 0.146	62.294	1.67
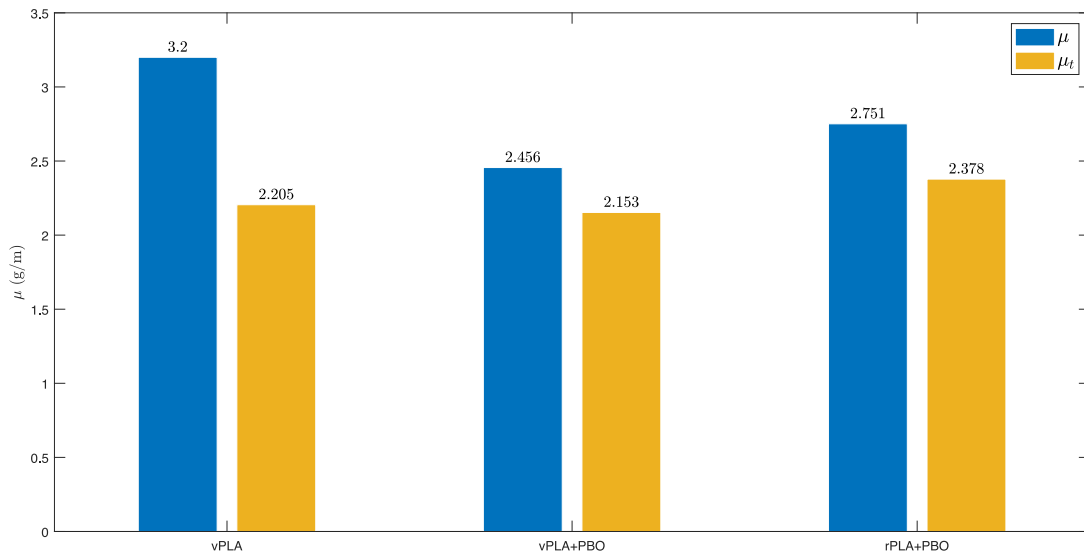
Figure 4.1: Linear mass density of the filament produced with the PLA formulations of each recycling chain.

between the vPLA and rPLA+PBO formulations, which may anticipate a decrease in melt strength that will be accessed with further testing.

4.2 Filament tensile tests

The results from the filament tensile tests (Table 4.2), illustrate that the vPLA filament tensile properties are substantially reduced when compared to similar tests conducted in the literature (see [76; 77]). This behavior is translated by a decrease in both tensile strength (83.38%) and elongation at break (61.70%) of vPLA filaments, when compared to the PLA control material used by Petchwattana *et al.* and can be explained can be explained by the effect of the melt-mixing and grinding steps. These additional processing steps were employed to the virgin polymer in order to normalize the degradation caused by these material preparation stages, therefore allowing to achieve comparable data about the extent of degradation between the pristine materials and the compatibilization of the PLA-based materials and the CE.

After chain extension the virgin PLA exhibited an increase in tensile modulus (33.5%), as well as a decrease in both ultimate tensile strength (19.8%) and elongation at break (19.7%) when compared to vPLA. These results suggest that the incorporation of PBO in the pristine PLA has a negative impact on its ultimate tensile properties, a behavior which can be associated to a low interaction between vPLA and the CE, as previously reported by Herrera *et al.* [53].

Recycled PLA (rPLA) presented a substantial decrease of tensile modulus (43.60%) and tensile strength (64.72%). However, the elongation at break exhibited a slight increase of ≈10%, when compared to the pristine material. In the presence of PBO, the recycled polymer partially recovers its mechanical properties, as observed by the increase in both tensile modulus (13%) and tensile strength (121%), when compared with rPLA.

Figure 4.2 presents the stress-strain curves for all the formulations of each recycling chain that highlight the fragile behavior of the material demonstrated by the absence of plastic deformation. The brittle nature of this grade of PLA represents the major constrain for the development of a multi-processing approach based on FFF, since the feedstock material for this technology has to be flexible enough in order to be continuously pushed by the machine towards the print head [70]. Moreover, the tendency for the recovery of the mechanical properties after chain extension is evident in the rPLA+PBO curve, which is in agreement with several reports from the literature [51; 62; 63].

4.3 Morphology

4.3.1 Surface morphology

The smooth surface of the neat PLA (Figure 4.3a) suggests a brittle fracture of the material, corroborating with literature [76], which was, in fact, confirmed by the filament tensile tests. Moreover, the white areas highlighted on the micrographs may represent some kind of inclusions that were trapped into the polymer matrix during processing, a behavior also reported by Brüster *et al* when analyzing plasticized PLA-based formulations [44] and which is in agreement with data from the linear mass density consistency analysis.

In the presence of PBO, (Figure 4.3b) the smooth surface was covered in peninsula-like layers and short uneven fibrils which are speculated to be a result of the reaction between the polymer and PBO, in agreement with the observations conducted by Tuna *et al.* on the fracture morphology of PLA/CE matrices [57]. Regarding the use of both recycled PLA and PBO, the formulation's microstructure presented a rougher and more heterogeneous surface than the pristine PLA-based materials, an observation which is in agreement with the reports by Badia *et al.* [43] and may be related to the decrease in mechanical performance, a hypothesis which was confirmed by the filament tensile tests.

4.3.2 Optical measurements

The incorporation of PBO on either virgin or recycled PLA did not significantly change the average luminosity of the samples, with the highest L^* value being observed for the rPLA+PBO sample (Table 4.3). On the other hand, a^* (red-green) and b^* (blue-yellow) color coordinates significantly change for the modified formulations, particularly
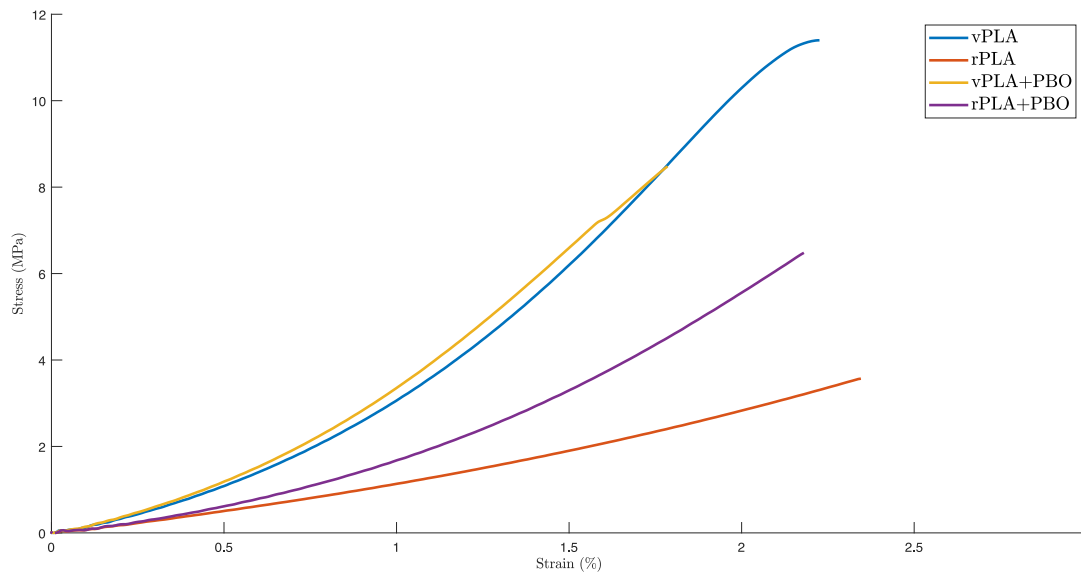
Figure 4.2: Stress-strain curves for the PLA formulations of each recycling chain, highlighting the recovery of the mechanical properties of recycled PLA after chain extension.

the b* color coordinate which represents a yellowing tendency of the polymer after the PBO incorporation, enhanced for the recycled PLA-based blend.

The tendency for PLA discoloration after melt processing has been described in the literature as a problem which adversely affects the properties and end use of the final products [78]. On the studied formulations, the yellowing was detected even in the control materials, which suggests that the color modifications may have resulted from some extent of oxidation that occurred during the melt-mixing stage. When in contact with the atmosphere, free radicals from the polymer's cleaved chains react with the oxygen to form new molecules, which, in turn, will absorb and reflect different wavelengths, therefore, leading to variations on color. Since reprocessed PLA is expected to have more cleaved chains available to react with the oxygen, this effect will be enhanced for recycled PLA-based materials, a behavior which is reflected by the evolution of the yellowness index, a standard parameter which describes the change in color from white towards yellow, and that was previously documented by Aguero *et al.* and Carrasco *et al* [42; 45]. The total difference in color measured by ΔE_{ab*} shows a noticeable variation in color in either vPLA+PBO and rPLA+PBO formulations when compared to the neat PLA.

4.4   Thermal behavior

The thermograms of the PLA-based formulations (Figure 4.4; Table 4.4) showed the presence of a first endothermic peak between 155 °C and 159 °C related to the PLA crystallization. Further, a single melting peak appeared in the temperature range between 173 °C and 175 °C. On the other hand, the neat PBO thermogram showed the presence of an endothermic peak around 148 °C associated with its melting phase transition.

From these results, an insignificant variation on the glass transition temperature between the virgin PLA and the compatibilized formulations was noticed, which is in
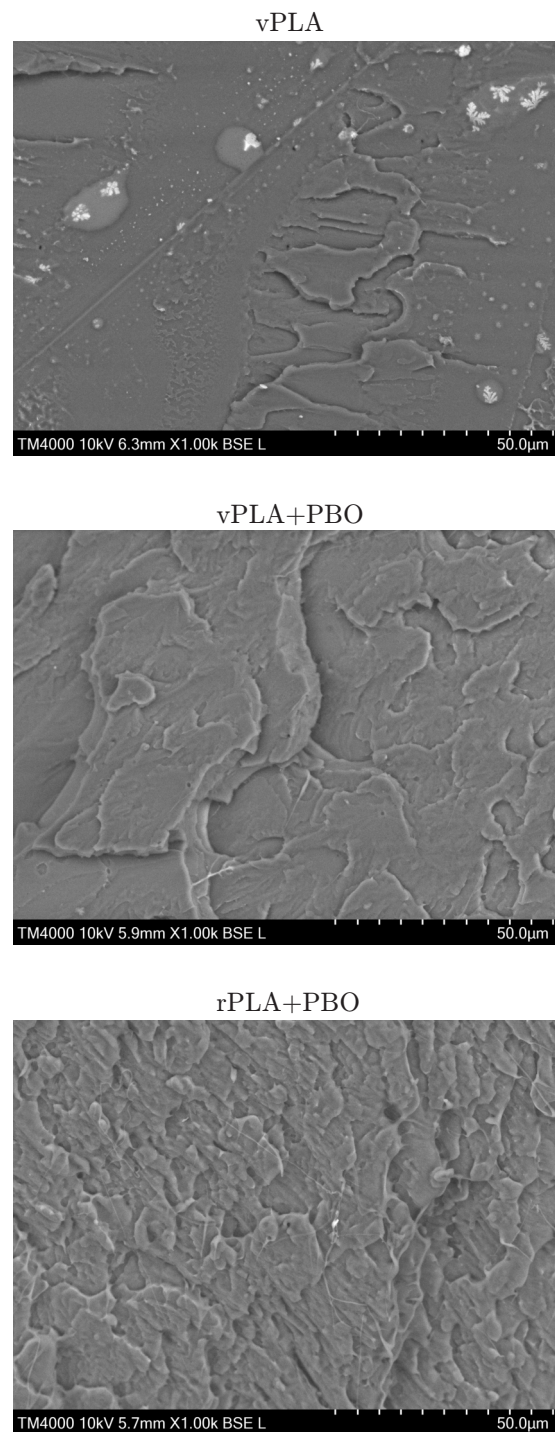
Figure 4.3: SEM micrographs representing the cross-sectional microstructure of the filament produced with vPLA; vPLA+PBO; and rPLA+PBO at a magnification of x1000.
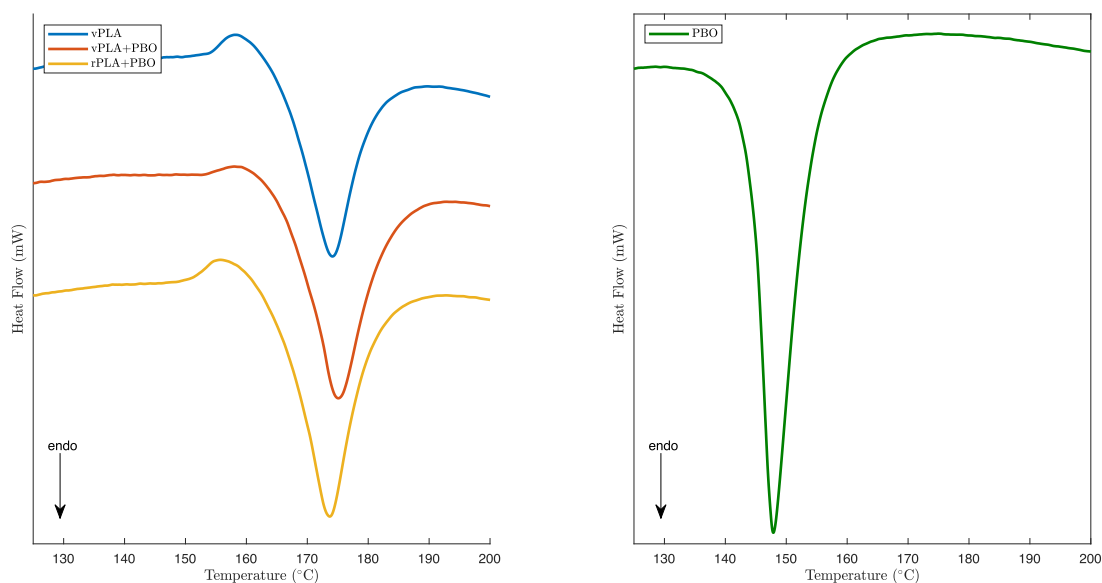
Figure 4.4: DSC thermograms recorded during the second heating of samples: PLA-based formulations (left); neat PBO (right).

agreement with several reports from the literature (see [42; 44; 46]). Similarly, the cold crystallization temperature (T_{cc}) did not significantly change, with exception for the rPLA+PBO formulation, which presented a slight decrease in T_{cc} when compared to the virgin polymer counterpart.

The determined melting temperature of vPLA was inferior to the one mentioned in the manufacturer's TDS. This behavior may be explained by the material preparation stages, particularly the melt mixing and grinding operations which were performed in order to normalize the degradation degreee between the virgin PLA and compatibilized formulations. However, among all the studied samples the melting transition did not significantly change, which allowed for the material to be processed at constant conditions.

From the analysis of the crystallization degree of the studied formulations, it was inferred that the amorphous domains tend to prevail more in the PLA formulations than crystalline ones [53] and PBO decreased PLA crystallinity. This particular observation suggests that PBO led to a more restrict mobility of the polymeric chain which, in turn, is unfavorable to the formation of orderly crystalline structures within the polymeric chains [51]. In contrast, an opposite result was expected for the recycled polymer, since the cleavage of the polymeric chains due to the chain scission phenomena would promote a higher mobility of these structures and, therefore, the formation of crystalline domains. In this context, the slight decrease on the degree of crystallinity between vPLA and rPLA+PBO may be an indicator of an effective chain extension, although further testing would be required to validate this hypothesis.

Table 4.2: Tensile properties of the filament produced with the different PLA formulations of each recycling chain.

	Tensile Modulus (MPa)	Tensile Strength (MPa)	Elongation at break (%)
vPLA	165.60 ± 7.38	11.45 ± 3.89	2.38 ± 0.64
rPLA	93.40 ± 16.61	4.04 ± 0.75	2.65 ± 0.44
vPLA+PBO	221.15 ± 9.33	9.18 ± 2.23	1.91 ± 0.34
rPLA+PBO	105.59 ± 23.92	8.93 ± 1.37	2.67 ± 0.41

Table 4.3: Average numbers for luminance (L^*), green-red (a^*), blue-yellow (b^*), total color difference (ΔE_{ab}^* and yellowness index (YI) for the neat PLA (vPLA) and modifed PLA with the chain extender (vPLA+PBO and rPLA+PBO).

	L^*	a^*	b^*	ΔE_{ab}^*	YI
vPLA	84.682 ± 0.921	0.556 ± 0.037	1.134 ± 0.160	-	32.915
vPLA+PBO	83.348 ± 0.957	0.090 ± 0.051	4.200 ± 0.400	3.376	37.415
rPLA+PBO	85.044 ± 0.854	0.266 ± 0.008	4.432 ± 0.464	3.330	37.858

Table 4.4: Thermal properties determined from the DSC thermograms for the different PLA-based formulations of each recycling chain.

	$\mathbf{T}_g$ (°C)	$\mathbf{T}_{cc}$ (°C)	$\mathbf{T}_m$ (°C)	$\chi(\%)$
vPLA	64.5	158.4	174.1	35.77
PBO	-	-	147.9	-
vPLA+PBO	66.2	159.1	175.0	24.28
rPLA+PBO	64	155.8	173.7	32.79

4.5   Structural analysis

By comparing the obtained FTIR spectra (Figure 4.5), the absence of modifications in the characteristic wavenumbers for PLA, particularly around 1745 cm^{-1} related to the presence of carbonyl groups (C=O), CH$_3$ deformation vibration at 1450 cm^{-1} and C-O stretching at 1180 cm^{-1} and 1078 cm^{-1}, as highlighted by the gray dashed lines, suggests that occurred low interaction between the PLA and PBO. Similar results were previously reported by Herrera *et al.* at this PBO concentration [53]. This behavior may be explained either by the CE's functionality, since PBO acts a as a di-functional chain extender, with two reactive sites, and, therefore, a higher concentration should be accounted for enhanced chain extension, or by the limited structural degradation of the formulation after processing (for virgin PLA-based materials) and reprocessing (for recycled PLA-based materials), which, although reflected by a decrease in mechanical performance and melt strength, can be insufficient to promote effective reaction with the PBO.

4.6   Melt flow rate

The MFR results (Figure 4.6) demonstrate that PLA's the MFR increased by ≈44% after its reprocessing without the chain extender. This behavior can be associated with a viscosity decrease that might have ocurred due to PLA molecular weight decrease, suggesting that the consecutive processing stages caused some extent of molecular degradation [42]. Moreover, the high standard deviation obtained for rPLA formulation indicates that the MFR values between replicates are more spread out, which can be associated to a shape factor of the 3D printed parts regrind used to perform the tests [79].

After the PBO incorporation, the MFR value for the virgin PLA was approximately the same, whereas the incorporation of the PBO in the recycled PLA led to an increase in the MFR by ≈21% when compared to the neat recycled polymer. These results are in disagreement with several reports from the literature, where the recovery of the molecular weight due to the reaction between the degraded polymer and the chain extender was translated into a significant decrease of the MFR [8; 51; 54; 64]. In this context, it can be speculated that this CE concentration is not enough to provide a recovery of the polymer's molecular weight and, therefore, of its melt strength. Moreover, the increase in the MFR between the rPLA and rPLA+PBO formulations can be explained by the melt mixing and grinding stages employed to the blend and which provide further thermo-mechanical degradation.

Finally, and although the obtained MFR results are not comparable to most of the literature or the manufacturer TDS due to the distinct test conditions, from the experimentation tests it could be concluded that this grade of PLA has a fluidity clearly beyond the theoretical processing window for a general 3D printing application. However, after performing a parametric optimization of 3D printer process parameters it is possible to set up the machine to mechanically push the filament at a rate which is compatible to its MFR, therefore assuring the material's printability.
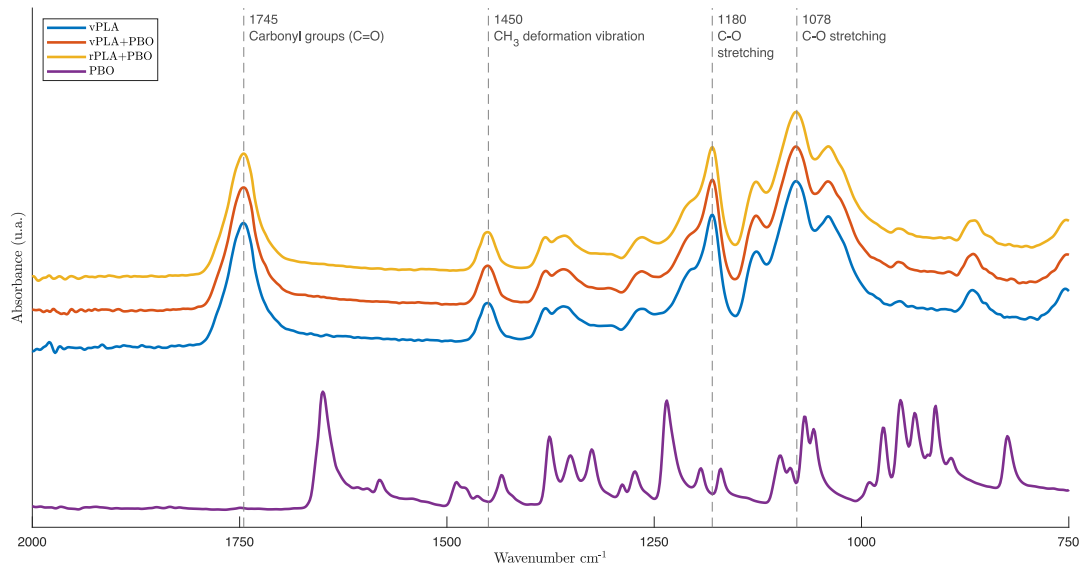
Figure 4.5: FTIR spectra for neat PLA (vPLA), chain extender (PBO) and the modified formulations of virgin and recycled PLA with the chain extender.
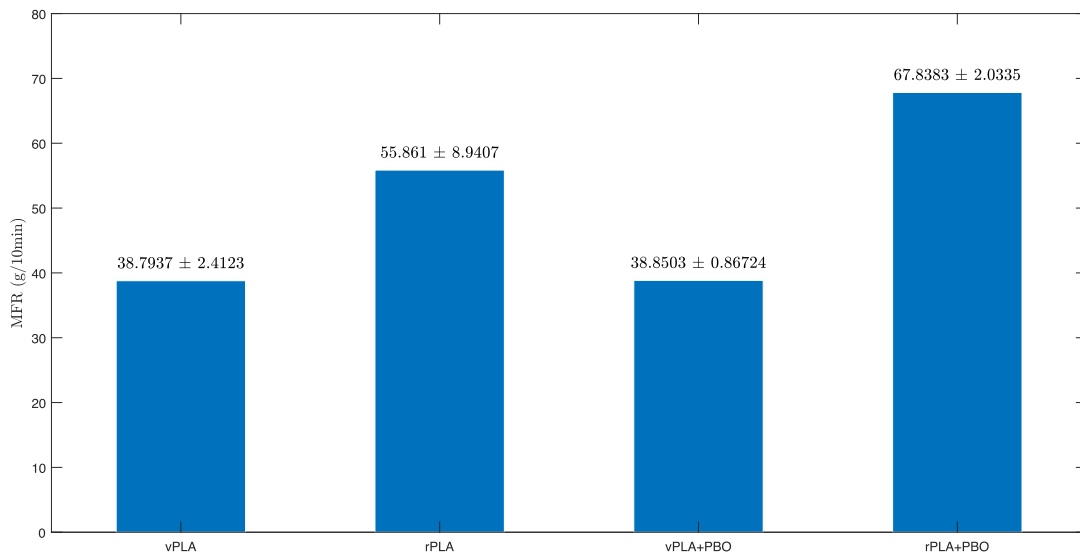

Figure 4.6: MFR of the melt extruded blends at 180°C and 1.2 kg load.

vPLA	vPLA+PBO	rPLA+PBO

Figure 4.7: Representation of the 3D components produced using virgin PLA (vPLA), virgin PLA and PBO (vPLA+PBO), and recycled PLA and PBO (rPLA+PBO) in order to conduct the qualitative printability test.

4.7 Printability test

The major limitation for the printability of each PLA-based formulation used was the brittle behavior of the material, corroborated by the filament tensile tests, and which contributed to the low success rate of the 3D printing stage, since the filament was prone to break before it could be fed into the 3D printer's nozzle. Moreover, filament spools from the different PLA formulations were not kept at controlled ambient conditions, which could have contributed to a brittle behavior, which became more evident over the course of the experimental work, particularly for the recycled polymer formulations.

From the components that could be completely or partially printed, virgin PLA-based formulations demonstrated the best 3D printing performance, with no evident signs of under or over extrusion and sufficient structural support to print the ≈20° overhangs of the regular dodecahedron without helpers (Figure 4.7). On the other hand, after mechanical recycling there was a shift in the ability to process the material through FFF technology. In fact, before chain extension (rPLA), the printability test was not able to be conducted due to the extreme brittleness of the filament. In turn rPLA+PBO allowed to obtain a 3D part, although it showed clear signs of under extrusion associated with segments of filament having inconsistent diameter, below the calculated average. Table 4.6 resumes the data obtained from the qualitative analysis of the print quality with the different PLA-based formulations.

4.8 FFF mechanical tests

Due to printability constraints, it was not possible to produce enough replicates to address the mechanical performance of the recycled PLA-based formulations and, therefore, only the results for vPLA and vPLA+PBO are presented (Table 4.5). Moreover, technological limitations regarding the testing equipment did not allow for the calculation of the tensile modulus for the given formulations.

The obtained results indicate that the incorporation of PBO into the virgin PLA

Table 4.5: Tensile properties of the specimens produced through FFF technology with PLA-based formulations from different recycling cycles.

	Tensile Modulus (MPa)	Tensile Strength (MPa)	Elongation at break (%)
vPLA	-	36.875 ± 0.625	4.885 ± 0.552
vPLA+PBO	-	37.188 ± 1.362	5.234 ± 1.306

did not affect its native mechanical performance, as reflected by the slight increase in the tensile strength (0.85%) and elongation at break (7.14%). The steadiness of the mechanical performance parameters between the control and the compatibilized formulation indicate a low interaction between PLA and the PBO, corroborating with the structural analysis and the MFR results, but not with the filament tensile tests data. This scenario may be explained by the fact that the methodology employed for the filament tensile tests is highly dependent on the test conditions, particularly the mounting tab design and the type of adhesive used to fix the specimen.

In sum, the experimental work conducted over the course of this research demonstrated that it is possible to successfully produce 3D printing filaments with all the formulations employed, including 100% recycled PLA (rPLA) and recycled-recovered PLA (rPLA+PBO). However, their property profile is clearly affected by the degradation mechanisms which result from the successive melt processing stages and mechanical recycling. In fact, tensile tests conducted to the filament demonstrate an evident decrease in mechanical properties of rPLA, when compared to its virgin polymer counterpart. After chain extension, the filament tensile properties seem to be partially recovered, a positive result which is in agreement with literature.

Moreover, optical measurements translate a yellowing experienced by the samples after the incorporation of the CE, although its influence does not significantly affect the polymer's structure, as demonstrated by the FTIR analysis. The processability of each of the formulations which was addressed through the MFR and printability tests demonstrated that, although the fluidity of this grade of PLA is clearly beyond the theoretical value to be employed in FFF applications, a parametric optimization of the process parameters does allow it to be printable. However, the brittle nature of the filament was identified as the main limitation for achieving an high rate success on the printability tests. In the following chapter the main conclusions gathered from experimental work are presented and future research work is suggested in order to better understand the possibility of successfully employ a closed-loop recycling scheme based on recycled-recovered PLA and FFF technology.

Table 4.6: Qualitative analysis of the print quality of the formulations of each recycling chain by addressing the success of the print, under or over extrusion, presence of voids and bubbles and layer shifts.

vPLA	The filament produced with the vPLA formulation was able to be printed, at the specified process parameters; Moreover, the resulting components did not show evident signs of under or over extrusion, voids and layer misalignment; However, some inclusions among the deposited beads were detected and the brittle behavior of the material led to a low 3D printing success rate; A regular dodecahedron and a set of tensile tests for accessing the mechanical performance of this formulation were able to be produced;
rPLA	100% recycled PLA was not able to be printed due to an extreme brittleness of the filament and, therefore, the printability analysis was not able to be conducted;
vPLA+PBO	After chain extension, virgin PLA was able to be printed at the same process parameters as the vPLA formulation; No evident signs of under or over extrusion, voids and layer misalignment were detected; However, due to the brittle nature of the filament only a partially printed dodecahedron was able to be produced, as well as a set of tensile specimens for accessing the mechanical performance of this formulation;
rPLA+PBO	After chain extension, recycled PLA was able to be printed at the same process parameters as the vPLA formulation; However, evident signs of under or over extrusion were detected, as well as the presence of voids and layer misalignment which were associated with the lower melt strength of this formulation; Moreover, due to embrittlement of the filament over time it was not possible to produce the set of tensile specimens required for accessing the mechanical performance of this formulation; A regular dodecahedron for the printability test was able to be produced;

Part V

Conclusions and future work

Chapter 5

Conclusions and Future work

5.1 Conclusions

The mechanical recycling revealed to have a negative effect on the material's mechanical performance and melt strength, as reflected by the decrease in the tensile modulus and tensile strength on the recycled PLA filaments and the MFR increase on the material, when compared to its virgin counterpart. After chain extension with PBO, recycled PLA partially recovered its mechanical performance, as reflected by an increase in both tensile modulus and tensile strength in the specimens, when compared to rPLA. However, PBO did not allow to recover the PLA melt strength. Moreover, vibrational spectroscopy of neat PLA and compatibilized formulations reflect a low interaction between the polymer and PBO. Further, the compatibilization between the virgin polymer and PBO did not significantly affect the mechanical performance and melt strength of the material, although of originating peninsula-like layers and some extent of fibrils in the material. Moreover, optical measurements reflected a noticeable discoloration, reflected by an yellowing of the virgin polymer after the PBO incorporation.

Regarding the processability of the material, filaments with consistent diameter were able to be produced with all the formulations obtained in each recycling chain. Moreover, a linear mass density consistency analysis was conducted by comparing the linear mass density computed through the ratio between the filament weight and the filament length and a theoretical counterpart based on the PLA density as stated on the manufacturer's TDS. This analysis allowed to understand that the vPLA filament was the most contaminated formulation by inclusions such as air bubbles or other contaminants, a result which was further corroborated by the surface morphology observations. For accessing the printability of the material, different components were produced through an open-source 3D printer. It was possible to print 3D parts with all the formulations of each recycling chain, except of the 100% recycled PLA. The brittle nature of the material represented the major constraint for either virgin polymer or compatibilized formulations, since the filament was prone to break in the extruder which led to a very low success rate in the 3D printing stage. In this context, it was not possible to establish a closed-loop recycling scheme by employing the developed methodology nor with the multi-processing approach to the virgin PLA or the virgin PLA/PBO and recycled-recovered PLA formulations.

Further, the incorporation of the chain extender as an upgrading strategy for

both virgin and recycled PLA led to inconclusive results, since on one hand recycled PLA after the chain extension seems to partially recover its mechanical performance, as reflected in the filament tensile tests, but, on the other hand, the MFR results, which provide an insight on the rheological properties of the material and, therefore, of the molecular weight of the polymer, demonstrate an increasing trend where a significant decrease was expected. In this context, further characterization of the chain extender should be considered in order to better understand how it reacts with the PLA and, therefore, enabling the definition of the optimum CE concentration which favors the PLA chain extension.

In sum, although the proposed objectives were not completely fulfilled, particularly the establishment of a methodology which enabled a closed-loop recycling scheme for additive manufacturing applications, the gathered conclusions provide a pathway for future work on the subjects of plastic reprocessing and upgrading strategies, as well as a guideline for PLA processing and testing conditions which is an important feature since PLA is not considered in most polymer testing standards.

5.2   Future work

In the aftermath of the present work, a set of possible research paths can be highlighted, particularly regarding the modification of the materials employed, different processing equipment and processing conditions, as well as the evaluation of different metrics which are fundamental to preserve not only the success of the processes involved but also the environmental commitment required through the contemporary standards.

In this context, the first logical research path is to understand how to modify this grade of PLA in order to make it suitable for replicating the proposed methodology. The application of additives such as plasticizers or impact modifiers could shift the fragile fracture of the material to a more ductile behavior and, therefore, making it suitable for extrusion-based applications. By using other grade of PLA, particularly extrusion grade PLA, a better set of results could be achieved.

Regarding the development of processing equipment, the modification of the cooling unit of the filament extruder by employing a multi-stage cooling could minimize the embrittlement of PLA during this process and, therefore, lead to the production of a filament of a higher quality. By using an industrial single screw extruder, equipped with a water bath multi-stage cooling system, the problematic associated with the inefficient cooling could be surpassed. After the filament production, keeping controlled temperature and relative humidity conditions, using a filament dryer or a similar equipment, is recommended.

Further characterization of PBO and testing the effect of its incorporation in recycled PLA at different concentrations by monitoring at least the modification of its structure, thermal, and rheological behavior could be a path to achieve the optimum concentration which favors the PLA chain extension.

Skipping the melt-mixing and subsequent grinding stages by blending the PLA and chain extender by reactive extrusion on a twin-screw extruder could be a path to minimize the thermomechanical degradation caused by these material preparation stages.

Finally, the influence of the chain extender on PLA compostability should be evaluated in order to ensure the preservation of its environmental friendly characteristics.

Intentionally blank page.

Bibliographic reference

[1] R. Geyer, J. R. Jambeck, and K. L. Law, "Production, use, and fate of all plastics ever made," *Science Advances*, vol. 3, no. 7, pp. 25–29, 2017.

[2] J. D. Badia and A. Ribes-Greus, "Mechanical recycling of polylactide, upgrading trends and combination of valorization techniques," *European Polymer Journal*, vol. 84, pp. 22–39, 2016. [Online]. Available: http://dx.doi.org/10.1016/j.eurpolymj.2016.09.005

[3] J. D. Badia, Ó. Gil-Castell, R. Teruel-Juanes, and A. Ribes-Greus, "Recycling of Polylactide," *Encyclopedia of Renewable and Sustainable Materials*, pp. 282–295, 2020.

[4] V. Piemonte, S. Sabatini, and F. Gironi, "Chemical Recycling of PLA: A Great Opportunity Towards the Sustainable Development?" *Journal of Polymers and the Environment*, vol. 21, no. 3, pp. 640–647, 2013.

[5] K. Ragaert, L. Delva, and K. Van Geem, "Mechanical and chemical recycling of solid plastic waste," *Waste Management*, vol. 69, pp. 24–58, 2017. [Online]. Available: https://doi.org/10.1016/j.wasman.2017.07.044

[6] F. Vilaplana and S. Karlsson, "Quality concepts for the improved use of recycled polymeric materials: A review," *Macromolecular Materials and Engineering*, vol. 293, no. 4, pp. 274–297, 2008.

[7] R. Khankrua, S. Pivsa-Art, H. Hiroyuki, and S. Suttiruengwong, "Effect of chain extenders on thermal and mechanical properties of poly(lactic acid) at high processing temperatures: Potential application in PLA/Polyamide 6 blend," *Polymer Degradation and Stability*, vol. 108, pp. 232–240, 2014. [Online]. Available: http://dx.doi.org/10.1016/j.polymdegradstab.2014.04.019

[8] W. Liu, H. Li, X. Wang, Z. Du, and C. Zhang, "Effect of chain extension on the rheological property and thermal behaviour of poly(lactic acid) foams," *Cellular Polymers*, vol. 32, no. 6, pp. 343–368, 2013.

[9] ISO/ASTM, "ISO/ASTM 52900: Additive manufacturing - General principles - Terminology," Tech. Rep., 2015. [Online]. Available: https://www.iso.org/obp/ui/#iso:std:69669:en%0Ahttps://www.iso.org/standard/69669.html%0Ahttps://www.astm.org/Standards/ISOASTM52900.htm

[10] B. Redwood, Ben; Schoffer, Filemon; Garret, *The 3D Printing Handbook*, D. Hubs, Ed. Amterdam: Coers Roest, 2013.

[11] J. Jordan, *3D Printing*, M. Press, Ed., Cambridge, MA, 2018.

[12] RePET, "About — RE PET 3D." [Online]. Available: https://re-pet3d.com/about/

[13] Filamentive, "About Us - Recycled 3D Printing Filament UK." [Online]. Available: https://www.filamentive.com/about-filamentive-recycled-filament/

[14] Reflow, "About – REFLOW." [Online]. Available: https://reflowproject.eu/about/

[15] Joana Azevedo, "Novo Filamento 3D produzido a partir de desperdícios de plástico dos makers — TUCAB." [Online]. Available: https://bit.ly/2VlaUqE

[16] T. Gomes, "Utilização de matéria prima secundária polimérica para aplicações em fabrico aditivo," Ph.D. dissertation, Universidade de Aveiro, 2013.

[17] F. A. Cruz Sanchez, H. Boudaoud, M. Camargo, and J. M. Pearce, "Plastic recycling in additive manufacturing: A systematic literature review and opportunities for the circular economy," *Journal of Cleaner Production*, vol. 264, 2020.

[18] BCN3D Technologies, "Introduction to Fused Filament Fabrication (FFF) 3D printing technology," Tech. Rep., 2019. [Online]. Available: https://bit.ly/2WtADO6

[19] M. Mensley, "3D Printer Extruder – The Ultimate Guide — All3DP," aug 2019. [Online]. Available: https://all3dp.com/1/3d-printer-extruder-nozzle-guide/

[20] J. P. M. Andias, "Incorporation of nanomaterials to customise recycled thermoplastics for applications in additive manufacturing," Ph.D. dissertation, Universidade de Aveiro, 2019.

[21] J. O'Connell, "FDM 3D Printers Explained: Cartesian, Delta, CoreXY, More — All3DP," 2020. [Online]. Available: https://all3dp.com/2/cartesian-3d-printer-delta-scara-belt-corexy-polar/

[22] Simplify3D, "Ultimate Materials Guide - Tips for 3D Printing with ABS," 2021. [Online]. Available: https://www.simplify3d.com/support/materials-guide/abs/

[23] M. von Übel, "3D Printing Materials Guide — All3DP," 2020. [Online]. Available: https://all3dp.com/1/3d-printing-materials-guide-3d-printer-material/

[24] AMFG, "The Additive Manufacturing Landscape 2020," Tech. Rep., 2020.

[25] ——, "Composite 3D Printing: An Emerging Technology with a Bright Future - AMFG," 2020. [Online]. Available: https://amfg.ai/2020/02/25/composite-3d-printing-an-emerging-technology-with-a-bright-future/

[26] S. Wickramasinghe, T. Do, and P. Tran, "FDM-Based 3D printing of polymer and associated composite: A review on mechanical properties, defects and treatments," *Polymers*, vol. 12, no. 7, pp. 1–42, 2020.

[27] X. Tian, T. Liu, Q. Wang, A. Dilmurat, D. Li, and G. Ziegmann, "Recycling and remanufacturing of 3D printed continuous carbon fiber reinforced PLA composites," *Journal of Cleaner Production*, vol. 142, pp. 1609–1618, 2017. [Online]. Available: http://dx.doi.org/10.1016/j.jclepro.2016.11.139

[28] Treatstock, "9 most common FDM 3D Printing Materials (Quick Simple Guide)," 2021. [Online]. Available: https://bit.ly/3ycvJCW

[29] A. Dey and N. Yodo, "A systematic survey of FDM process parameter optimization and their influence on part characteristics," *Journal of Manufacturing and Materials Processing*, vol. 3, no. 3, 2019.

[30] Simplify3D, "Ultimate 3D Printing Material Properties Table," 2021. [Online]. Available: https://www.simplify3d.com/support/materials-guide/properties-table/

[31] J. R. Wagner, E. M. Mount, and H. F. Giles, *Extrusion: The Definitive Processing Guide and Handbook: Second Edition*, 2013.

[32] D. V. Rosato, *Extruding Plastics*, Dordrecht, 1998.

[33] J. O'Connell, "How Is 3D Printer Filament Made? — All3DP," 2020. [Online]. Available: https://all3dp.com/2/how-3d-printer-filament-made/

[34] M. E. Grigore, "Methods of recycling, properties and applications of recycled thermoplastic polymers," *Recycling*, vol. 2, no. 4, pp. 1–11, 2017.

[35] E. Hopewell, Jefferson; Dvorak, Robert; Kosior, "Plastic Recycling - Challenges and Oportunities," *Philosophical Transactions of the Royal society*, vol. B, no. 364, pp. 2115–2126, 2009.

[36] S. M. Al-Salem, P. Lettieri, and J. Baeyens, "Recycling and recovery routes of plastic solid waste (PSW): A review," *Waste Management*, vol. 29, no. 10, pp. 2625–2643, 2009. [Online]. Available: http://dx.doi.org/10.1016/j.wasman.2009.06.004

[37] I. Pillin, N. Montrelay, A. Bourmaud, and Y. Grohens, "Effect of thermo-mechanical cycles on the physico-chemical properties of poly(lactic acid)," *Polymer Degradation and Stability*, vol. 93, no. 2, pp. 321–328, 2008.

[38] M. Zenkiewicz, J. Richert, P. Rytlewski, K. Moraczewski, M. Stepczyńska, and T. Karasiewicz, "Characterisation of multi-extruded poly(lactic acid)," *Polymer Testing*, vol. 28, no. 4, pp. 412–418, 2009.

[39] F. A. Cruz Sanchez, H. Boudaoud, S. Hoppe, and M. Camargo, "Polymer recycling in an open-source additive manufacturing context: Mechanical issues," *Additive Manufacturing*, vol. 17, pp. 87–105, 2017. [Online]. Available: https://doi.org/10.1016/j.addma.2017.05.013

[40] A. A. Cuadri and J. E. Martín-Alfonso, "Thermal, thermo-oxidative and thermomechanical degradation of PLA: A comparative study based on rheological, chemical and thermal properties," *Polymer Degradation and Stability*, vol. 150, pp. 37–45, 2018. [Online]. Available: https://doi.org/10.1016/j.polymdegradstab.2018.02.011

[41] S. Inkinen, M. Hakkarainen, A. C. Albertsson, and A. Södergård, "From lactic acid to poly(lactic acid) (PLA): Characterization and analysis of PLA and Its precursors," *Biomacromolecules*, vol. 12, no. 3, pp. 523–532, 2011.

[42] F. Carrasco, P. Pagès, J. Gámez-Pérez, O. O. Santana, and M. L. Maspoch, "Processing of poly(lactic acid): Characterization of chemical structure, thermal stability and mechanical properties," *Polymer Degradation and Stability*, vol. 95, no. 2, pp. 116–125, 2010.

[43] J. D. Badia, E. Strömberg, S. Karlsson, and A. Ribes-Greus, "Material valorisation of amorphous polylactide. Influence of thermo-mechanical degradation on the morphology, segmental dynamics, thermal and mechanical performance," *Polymer Degradation and Stability*, vol. 97, no. 4, pp. 670–678, 2012. [Online]. Available: http://dx.doi.org/10.1016/j.polymdegradstab.2011.12.019

[44] B. Brüster, F. Addiego, F. Hassouna, D. Ruch, J. M. Raquez, and P. Dubois, "Thermo-mechanical degradation of plasticized poly(lactide) after multiple reprocessing to simulate recycling: Multi-scale analysis and underlying mechanisms," *Polymer Degradation and Stability*, vol. 131, pp. 132–144, 2016. [Online]. Available: http://dx.doi.org/10.1016/j.polymdegradstab.2016.07.017

[45] A. Agüero, M. d. C. Morcillo, L. Quiles-Carrillo, R. Balart, T. Boronat, D. Lascano, S. Torres-Giner, and O. Fenollar, "Study of the influence of the reprocessing cycles on the final properties of polylactide pieces obtained by injection molding," *Polymers*, vol. 11, no. 12, pp. 1–20, 2019.

[46] L. Botta, R. Scaffaro, F. Sutera, and M. C. Mistretta, "Reprocessing of PLA/graphene nanoplatelets nanocomposites," *Polymers*, vol. 10, no. 1, 2018.

[47] F. R. Beltrán, V. Lorenzo, M. U. de la Orden, and J. Martínez-Urreaga, "Effect of different mechanical recycling processes on the hydrolytic degradation of poly(L-lactic acid)," *Polymer Degradation and Stability*, vol. 133, no. 2016, pp. 339–348, 2016.

[48] Y. L. Jiun, C. T. Tze, U. Moosa, and M. A. Tawawneh, "Effects of recycling cycle on used thermoplastic polymer and thermoplastic elastomer polymer," *Polymers and Polymer Composites*, vol. 24, no. 9, pp. 735–740, 2016.

[49] V. Frenz, D. Scherzer, M. Villalobos, A. A. Awojulu, M. Edison, and R. Van Der Meer, "Multifunctional polymers as chain extenders and compatibilizers for polycondensates and biopolymers," *Technical Papers, Regional Technical Conference - Society of Plastics Engineers*, vol. 3, no. July, pp. 1678–1682, 2008.

[50] R. Scaffaro, M. Morreale, F. Mirabella, and F. P. La Mantia, "Preparation and recycling of plasticized PLA," *Macromolecular Materials and Engineering*, vol. 296, no. 2, pp. 141–150, 2011.

[51] M. Barletta, C. Aversa, and M. Puopolo, "Recycling of PLA-based bioplastics: The role of chain-extenders in twin-screw extrusion compounding and cast extrusion of sheets," *Journal of Applied Polymer Science*, vol. 137, no. 42, 2020.

[52] L. Aliotta, P. Cinelli, M. B. Coltelli, M. C. Righetti, M. Gazzano, and A. Lazzeri, "Effect of nucleating agents on crystallinity and properties of poly (lactic acid) (PLA)," *European Polymer Journal*, vol. 93, pp. 822–832, 2017. [Online]. Available: http://dx.doi.org/10.1016/j.eurpolymj.2017.04.041

[53] C. A. Ramírez-Herrera, A. I. Flores-Vela, A. M. Torres-Huerta, M. A. Domínguez-Crespo, and D. Palma-Ramírez, "PLA degradation pathway obtained from direct polycondensation of 2-hydroxypropanoic acid using different chain extenders," *Journal of Materials Science*, vol. 53, no. 15, pp. 10 846–10 871, 2018.

[54] M. A. Ghalia and Y. Dahman, "Investigating the effect of multi-functional chain extenders on PLA/PEG copolymer properties," *International Journal of Biological Macromolecules*, vol. 95, pp. 494–504, 2017.

[55] J. M. Julien, J. C. Quantin, J. C. Bénézet, A. Bergeret, M. F. Lacrampe, and P. Krawczak, "Chemical foaming extrusion of poly(lactic acid) with chain-extenders: Physical and morphological characterizations," *European Polymer Journal*, vol. 67, pp. 40–49, 2015. [Online]. Available: http://dx.doi.org/10.1016/j.eurpolymj.2015.03.011

[56] N. Najafi, M. C. Heuzey, P. J. Carreau, and P. M. Wood-Adams, "Control of thermal degradation of polylactide (PLA)-clay nanocomposites using chain extenders," *Polymer Degradation and Stability*, vol. 97, no. 4, pp. 554–565, 2012.

[57] B. Tuna and G. Ozkoc, "Effects of Diisocyanate and Polymeric Epoxidized Chain Extenders on the Properties of Recycled Poly(Lactic Acid)," *Journal of Polymers and the Environment*, vol. 25, no. 4, pp. 983–993, 2017.

[58] BASF, "Polymeric Chain Extenders Joncry ADR-4368 Data Sheet," Tech. Rep., 2008.

[59] X. Meng, G. Shi, W. Chen, C. Wu, Z. Xin, T. Han, and Y. Shi, "Structure effect of phosphite on the chain extension in PLA," *Polymer Degradation and Stability*, vol. 120, pp. 283–289, 2015. [Online]. Available: http://dx.doi.org/10.1016/j.polymdegradstab.2015.07.019

[60] X. Meng, G. Shi, C. Wu, W. Chen, Z. Xin, Y. Shi, and Y. Sheng, "Chain extension and oxidation stabilization of Triphenyl Phosphite (TPP) in PLA," *Polymer Degradation and Stability*, vol. 124, pp. 112–118, 2016. [Online]. Available: http://dx.doi.org/10.1016/j.polymdegradstab.2015.12.003

[61] T. Han, Z. Xin, Y. Shi, S. Zhao, X. Meng, H. Xu, and S. Zhou, "Control of thermal degradation of poly(lactic acid) using functional polysilsesquioxane microspheres as chain extenders," *Journal of Applied Polymer Science*, vol. 132, no. 20, pp. 1–11, 2015.

[62] D. Rasselet, A. S. Caro-Bretelle, A. Taguet, and J. M. Lopez-Cuesta, "Reactive compatibilization of PLA/PA11 blends and their application in additive manufacturing," *Materials*, vol. 12, no. 3, 2019.

[63] M. T. Alturkestany, V. Panchal, and M. R. Thompson, "Improved part strength for the fused deposition 3D printing technique by chemical modification of polylactic acid," *Polymer Engineering and Science*, vol. 59, no. s2, pp. E59–E64, 2019.

[64] Y. Baimark and P. Srihanam, "Influence of chain extender on thermal properties and melt flow index of stereocomplex PLA," *Polymer Testing*, vol. 45, pp. 52–57, 2015.

[65] M. A. Vigil Fuentes, S. Thakur, F. Wu, M. Misra, S. Gregori, and A. K. Mohanty, "Study on the 3D printability of poly(3-hydroxybutyrate-co-3-hydroxyvalerate)/poly(lactic acid) blends with chain extender using fused filament fabrication," *Scientific Reports*, vol. 10, no. 1, pp. 1–12, 2020. [Online]. Available: https://doi.org/10.1038/s41598-020-68331-5

[66] E. O. Cisneros-López, A. K. Pal, A. U. Rodriguez, F. Wu, M. Misra, D. F. Mielewski, A. Kiziltas, and A. K. Mohanty, "Recycled poly(lactic acid)–based 3D printed sustainable biocomposites: a comparative study with injection molding," *Materials Today Sustainability*, vol. 7-8, pp. 1–12, 2020.

[67] C. Cardona, A. H. Curdes, and A. J. Isaacs, "Effects of Filament Diameter Tolerances in Fused Filament Fabrication," *IU Journal of Undergraduate Research*, vol. 2, no. 1, pp. 44–47, 2016.

[68] N. E. Zander, M. Gillan, and R. H. Lambeth, "Recycled polyethylene terephthalate as a new FFF feedstock material," *Additive Manufacturing*, vol. 21, no. January, pp. 174–182, 2018. [Online]. Available: https://doi.org/10.1016/j.addma.2018.03.007

[69] M. E. Mackay, "The importance of rheological behavior in the additive manufacturing technique material extrusion," *Journal of Rheology*, vol. 62, no. 6, pp. 1549–1561, 2018. [Online]. Available: http://dx.doi.org/10.1122/1.5037687

[70] X. G. Zhao, K. J. Hwang, D. Lee, T. Kim, and N. Kim, "Enhanced mechanical properties of self-polymerized polydopamine-coated recycled PLA filament used in 3D printing," *Applied Surface Science*, vol. 441, pp. 381–387, 2018. [Online]. Available: https://doi.org/10.1016/j.apsusc.2018.01.257

[71] ASTM D1238, "Standard Test Method for Melt Flow Rates of Thermoplastics by Extrusion Plastometer," Tech. Rep. 8, 2014.

[72] Stable Micro Systems, "Tips and tricks for successful tensile testing: Stretching the boundaries in your lab," 2015.

[73] ISO 14026, "International Standard International Standard," *61010-1 © Iec:2001*, vol. 2014, p. 13, 2014.

[74] Wanner Technik GmbH, "Compact - Wanner Technik GmbH." [Online]. Available: https://www.wanner-technik.de/en/granulators/compact/

[75] I. Gonçalves, J. Lopes, A. Barra, D. Hernández, C. Nunes, K. Kapusniak, J. Kapusniak, D. V. Evtyugin, J. A. Lopes da Silva, P. Ferreira, and M. A. Coimbra, "Tailoring the surface properties and flexibility of starch-based films using oil and waxes recovered from potato chips byproducts," *International Journal of Biological Macromolecules*, vol. 163, pp. 251–259, 2020. [Online]. Available: https://doi.org/10.1016/j.ijbiomac.2020.06.231

[76] N. Petchwattana, W. Channuan, P. Naknaen, and B. Narupai, "3D printing filaments prepared from modified poly(lactic acid)/teak wood flour composites: An investigation on the particle size effects and silane coupling agent compatibilisation," *Journal of Physical Science*, vol. 30, no. 2, pp. 169–188, 2019.

[77] A. Costa, "Nanocompósitos de matriz polimérica para impressão 3D," Ph.D. dissertation, Universidade de Aveiro, 2016.

[78] C. M. B. Goncalves, J. A. P. Coutinho, and I. M. Marrucho, "Optical properties of polylactic acid," in *Poly(lactic acid): Synthesis, Structures, Properties, Processing, and Applications*, H. Auras, Rafael; Lim, Loong-Tak; Selke, Susan E. M.; Tsuji, Ed. John Wiley Sons, 2010, ch. 8, pp. 97–113.

[79] N. Singh, R. Singh, and I. P. Ahuja, "Recycling of polymer waste with SiC/Al2O3 reinforcement for rapid tooling applications," *Materials Today Communications*, vol. 15, no. January, pp. 124–127, 2018. [Online]. Available: https://doi.org/10.1016/j.mtcomm.2018.02.008